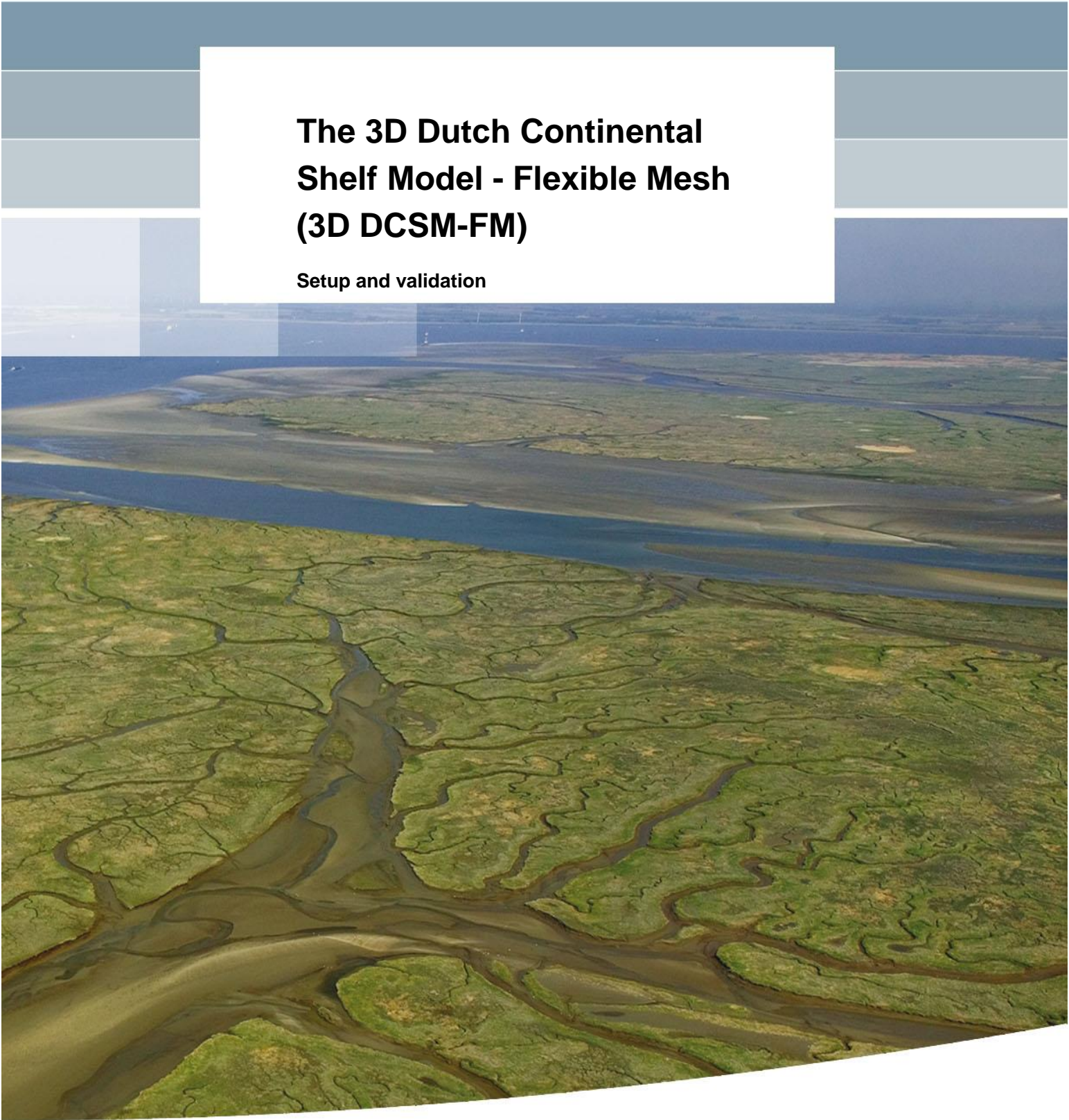


**The 3D Dutch Continental
Shelf Model - Flexible Mesh
(3D DCSM-FM)**

Setup and validation



The 3D Dutch Continental Shelf Model - Flexible Mesh (3D DCSSM- FM)

Setup and validation

Firmijn Zijl
Jelmer Veenstra
Julien Groenenboom

1220339-000

Title

The 3D Dutch Continental Shelf Model - Flexible Mesh (3D DCSM-FM)

Client

RWS-WVL

Project

1220339-000

Reference

1220339-000-ZKS-0042

Pages

41

Keywords

Coastal Genesis, Numerical Modelling, North Sea, NW European Continental Shelf, Delft3D Flexible Mesh, Hydrodynamics


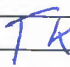

Summary

This report deals with the setup and validation of a three-dimensional hydrodynamic model (3D DCSM-FM) of the Northwest European Shelf, including the North Sea and adjacent shallow seas and estuaries such as the Wadden Sea and the Eastern and Western Scheldt.

The model is developed in D-HYDRO Flexible Mesh and is based on the horizontal schematization of the 2D DCSM-FM model. Unlike this 2D model, 3D DCSM-FM includes temperature and salinity as state parameters. The validation is performed for three configurations of the model, which differ from each other with respect to horizontal resolution, model bathymetry and bottom roughness.

Based on hindcast simulations covering the years 2006-2012 and 2013-2017 these configurations have been validated with respect to:

- water levels in Dutch coastal waters,
- sea surface temperature in the ,
- temperature stratification in the central North Sea,
- mean cross-shore surface salinity gradients in the Rhine ROFI,
- residual transport through the English Channel and
- current velocities 27-28 km off the Egmond coast and near Ameland.

Version	Date	Author	Initials	Review	Initials	Approval	Initials
memo	may 2018	Firmijn Zijl		Theo van der Kaaij		Frank Hoozemans	
final	July 2018	Firmijn Zijl		Theo van der Kaaij		Frank Hoozemans	

State

final

Contents

1	Introduction	1
1.1	Background Kustgenese 2	1
1.2	Objective and scope	1
1.3	Model versions	2
1.4	Outline of the report	2
2	Description of the 3D DCSM-FM model	3
2.1	Network	3
2.2	Bathymetry	4
2.3	Bottom roughness	6
2.4	Open boundary conditions	6
2.5	Meteorological forcing	7
2.5.1	Wind and pressure forcing	7
2.5.2	Heat-flux model and forcing	8
2.6	River discharges	8
2.7	Miscellaneous	9
2.7.1	Tidal potential	9
2.7.2	Horizontal viscosity	9
2.7.3	Initial conditions and spin-up period	9
2.7.4	Time zone	9
2.7.5	Computational time	9
3	Model validation: water levels	10
4	Model validation: water temperature	13
4.1	Sea surface temperature	13
4.2	Temperature stratification in the central North Sea	15
5	Model validation: sea surface salinity	18
6	Residual transport through the English Channel	21
7	Comparison with observed flow velocities	23
7.1	Introduction	23
7.1	Data availability	23
7.1.1	Selected data	24
7.2	HKZ A/B	26
7.2.1	Visual comparison	26
7.2.2	Quantitative comparison	27
7.2.3	Variation over depth	29
7.3	Kustgenese 2 Ameland data	31
7.3.1	Visual comparison	31
7.3.2	Quantitative comparison	33
7.3.3	Variation over depth	35
8	Conclusions and recommendations	38
8.1	Conclusions	38

8.2 Recommendations	39
References	41

1 Introduction

1.1 Background Kustgenese 2

Dutch coastal policy aims for a safe, economically strong and attractive coast. This is achieved by maintaining the part of the coast that support these functions; the coastal foundation. The coastal foundation is maintained by means of sand nourishments; the total nourishment volume is approximately 12 million m³/year since 2000.

In 2020 the Dutch Ministry of Infrastructure and Environment will make a decision on the nourishment volume. The Kustgenese-2 (KG2) programme is aimed to deliver knowledge to enable this decision making. The scope of the KG2 project commissioned by Rijkswaterstaat to Deltares is determined by two main questions:

- 1 What are possibilities for an alternative offshore boundary of the coastal foundation?
- 2 How much sediment is required for the coastal foundation to grow with sea level rise?

The Deltares KG2 subproject “Diepere Vooroever” (DV, lower shoreface) contributes to both questions. The KG2-DV project studies the morphodynamics of the Dutch lower shoreface, in particular the net cross-shore sand transport as function of depth on the basis of field measurements, numerical modelling and system knowledge.

1.2 Objective and scope

The study focusses on the Dutch lower shoreface which is defined as the area between the upper shoreface (with regular and dominant wave action) and the shelf (no serious wave action). This is roughly the zone between the outer breaker bar (approx. NAP -8 m) and the NAP -20 m depth contour. The latter has been defined as the offshore boundary of the coastal foundation (Lodder, 2016).

Current profiles computed with a hydrodynamic model are required for subsequent sediment transport computations, with the eventual aim to assess the annual sediment transport rates across the offshore boundary of the coastal foundation. The hydrodynamic model that is used is the 3D Dutch Continental Shelf Model developed in D-HYDRO Flexible Mesh (3D DCSM-FM).

This report describes the model setup and validation of the 3D DCSM-FM model. This mainly concerns work that is funded through other projects, e.g. Deltares’ own strategic research funding. For sediment transport, the variation of the velocity profile over the water column is relevant, since strong velocities near the bottom cause bed load transport and stir up sediment for the suspended transport. Therefore, within the Kustgenese 2 project work an additional validation of 3D DCSM-FM against current measurements was performed. The other validation work concerns water levels (tide and surge), sea surface temperature, temperature stratification, surface salinity gradients in the Rhine ROFI and residual transport through the English Channel.

In Grasmeyer (2018) the method to compute the sediment transport rates on the Dutch lower shoreface is presented. This method is based on long-term hydrodynamic computations with 3D DCSM-FM.

1.3 Model versions

3D DCSM-FM is originally setup as part of Deltares' strategic research funding, with a focus on long-term water quality. Since then this model has been used for numerous studies. This configuration of 3D DCSM-FM is originally based on the fifth generation WAQUA DCSMv6 and is referred to in this report as the 'original' configuration.

Separately, a sixth generation 2D DCSM Flexible Mesh model is being developed for Rijkswaterstaat (Zijl and Groenenboom, 2017). One of the main advantages of this schematization is that the bathymetry is based on an improved data product (EMODnet; previously NOOS). This has removed the need to adjust the model bathymetry during the model calibration, as was required during the development of DCSMv6 (Zijl et al., 2018). While this adjustment was beneficial for the skill with which water levels are represented, it is unclear what the impact on current velocities is. Therefore, two additional versions of 3D DCSM-FM were setup. These are partially based on preliminary versions of the 2D DCSM-FM sixth generation model with improved unadjusted bathymetry and are referred to in this report as the '1 nm' configuration and the '0.5 nm' configuration, reflecting the highest horizontal grid resolution that is present in the model (nm = nautical mile, 1.85 km).

Only the setup of the '0.5 nm' configuration of the model is described in this report, even though in the validation all three versions of the model ('original', '1 nm' and '0.5 nm') are used and compared.

1.4 Outline of the report

Chapter 2 describes the setup of the 0.5 nm configuration of 3D DCSM-FM. Chapter 3, 4 and 5 deal with model validation with respect to water levels, water temperature and sea surface salinity, respectively. In Chapter 6 the residual currents through the English Channel are assessed and in Chapter 7, the model is validated against current measurements.

2 Description of the 3D DCSM-FM model

2.1 Network

The model network of 3D DCSM-FM covers the northwest European continental shelf, specifically the area between 15° W to 13° E and 43° N to 64° N (e.g. Figure 2.1). This means that the open boundary locations are the same as in DCSMv6. The computational grid of the previous generation WAQUA-DCSMv6 model has rectangular cells with a uniform resolution. One of the advantages of D-HYDRO above WAQUA is the enhanced possibility to better match resolution with relevant local spatial scales.

The advantage of coarsening in deep areas in particular is twofold: firstly it reduces the number of cells in areas where local spatial scales allow it and secondly it eases the numerical time step restriction. The combination of both lead to a reduction in computational time with a factor ~4, while – crucially – maintaining accuracy in terms of water level representation.

The DCSM-FM network was designed to have a resolution that increases with decreasing water depth. The starting point was a network with a uniform cell size of 1/10° in east-west direction and 1/15°. This coarse network was refined in three steps with a factor of 2 by 2. The areas of refinement were specified with smooth polygons that were approximately aligned with the 800 m, 200m, 50 m and 12.5 m isobaths (i.e., lines with equal depth). Areas with different resolution are connected with triangles. The choice of isobaths ensures that the cell size scales with the square root of the depth, resulting in relatively limited variations of wave Courant number within the model domain.

An exception was made for the southern North Sea, where the area of highest resolution was expanded. This was done to ensure that the highly variable features in the bathymetry can properly be represented on the network. Furthermore, it ensures that the areas where steep salinity gradients can be expected are within the area with the highest resolution.

The resulting network is shown in Figure 2.1 and has approximately 630,000 cells with a variable resolution. The largest cells (shown in yellow) have a size of 1/10° in east-west direction and 1/15° in north-south direction, which corresponds to about 4 x 4 nautical miles (nm) or 4.9-8.1 km by 7.4 km, depending on the latitude. The smallest cells (shown in red) have a size of 2/3' in east-west direction and 1/2' in north-south direction. This corresponds to about 0.5 nm x 0.5 nm or 840 m x 930 m in the vicinity of the Dutch waters.

The network is specified in geographical coordinates (WGS84).

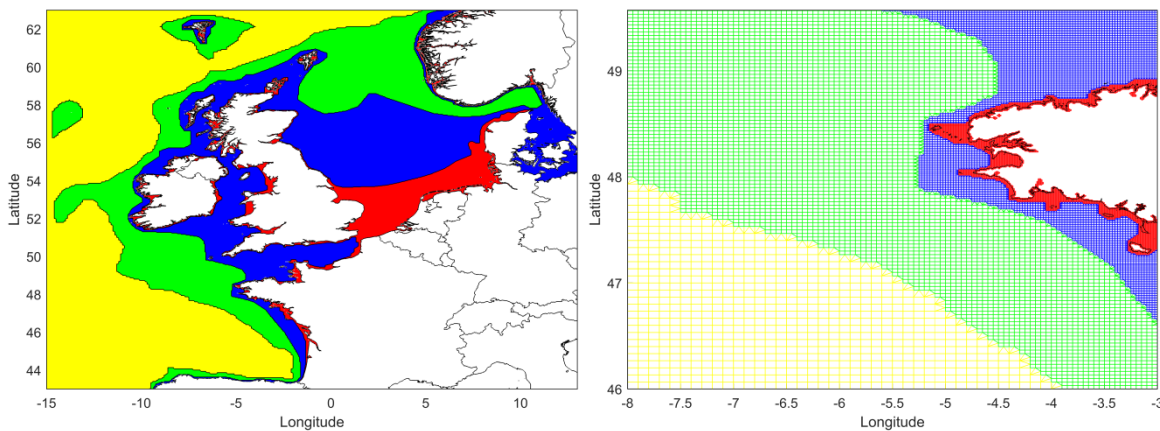


Figure 2.1 Overview (left) and detail (right) of the DCSM-FM model network with the colours indicating the grid size (yellow: ~ 4 nm; green: ~ 2 nm; blue: ~ 1 nm; red: ~ 0.5 nm).

Vertical schematization

For the 3D DCSM-FM model the sigma-layer approach is used for the vertical schematization. This implies that the water column is divided into a fixed number of layers, independent of the local water depth. Consequently, the vertical resolution increases in shallow areas and changes because of water level variations in both space and time. A total of 20 layers with a uniform thickness of 5 % of the local water depth are applied. This is expected to be sufficient for relatively shallow coastal areas. However, to correctly represent processes in deeper water and along the shelf edge, other vertical schematizations and layer distributions should be considered. One idea to investigate is to use a combination of sigma-layers for the upper part of the water column and strictly horizontal z-layers for the lower part.

2.2 Bathymetry

The DCSM-FM model bathymetry has been derived from a gridded bathymetric dataset from the European Marine Observation and Data Network (EMODnet), a consortium of organisations assembling European marine data, metadata and data products from diverse sources. The data are compounded from selected bathymetric survey data sets (single and multi-beam surveys) and composite DTMs, while gaps with no data coverage are completed by integrating the GEBCO 30'' gridded bathymetry.

The resolution of the gridded EMODnet dataset is $1/8' \times 1/8'$ (approx. 160×230 m). For interpolation, the average of the surrounding data points was used, within a search radius equal to the cell size.

LAT-MSL realization

The EMODnet data is only provided relative to Lowest Astronomical Tide (LAT). To make these data applicable for DCSM-FM, we have converted to the Mean Sea Level (MSL) vertical reference plane. The LAT-MSL relation was derived from a 19-year tide-only simulation with the previous generation DCSMv6.

Baseline bathymetry

For large parts of the Dutch waters there is also Baseline bathymetry data available. Where applicable this has been used. Note that the Baseline bathymetry is referenced to NAP, while after conversion the EMODnet data was referenced to MSL.

The model bathymetry is provided on the net nodes. Depths at the middle of the cell edges (the velocity points) are set to be determined as the mean value of the depth at the adjacent nodes. Depths at the location of the cell face (the water level points) are specified to be determined as the maximum of the depth in the surrounding cell edges.

An overview of the resulting DCSM-FM model bathymetry is presented in Figure 2.2. This shows that depths of more than 2000 m occur in the northern parts of the model domain, with depths exceeding 5000 m in the south-western part. The North Sea is much shallower with depths rarely exceeding 100m in the central and southern part. In Figure 2.3 a detail of the DCSM-FM model bathymetry is shown focussing on the southern North Sea. In the southern North Sea depths are generally less than 50 m.

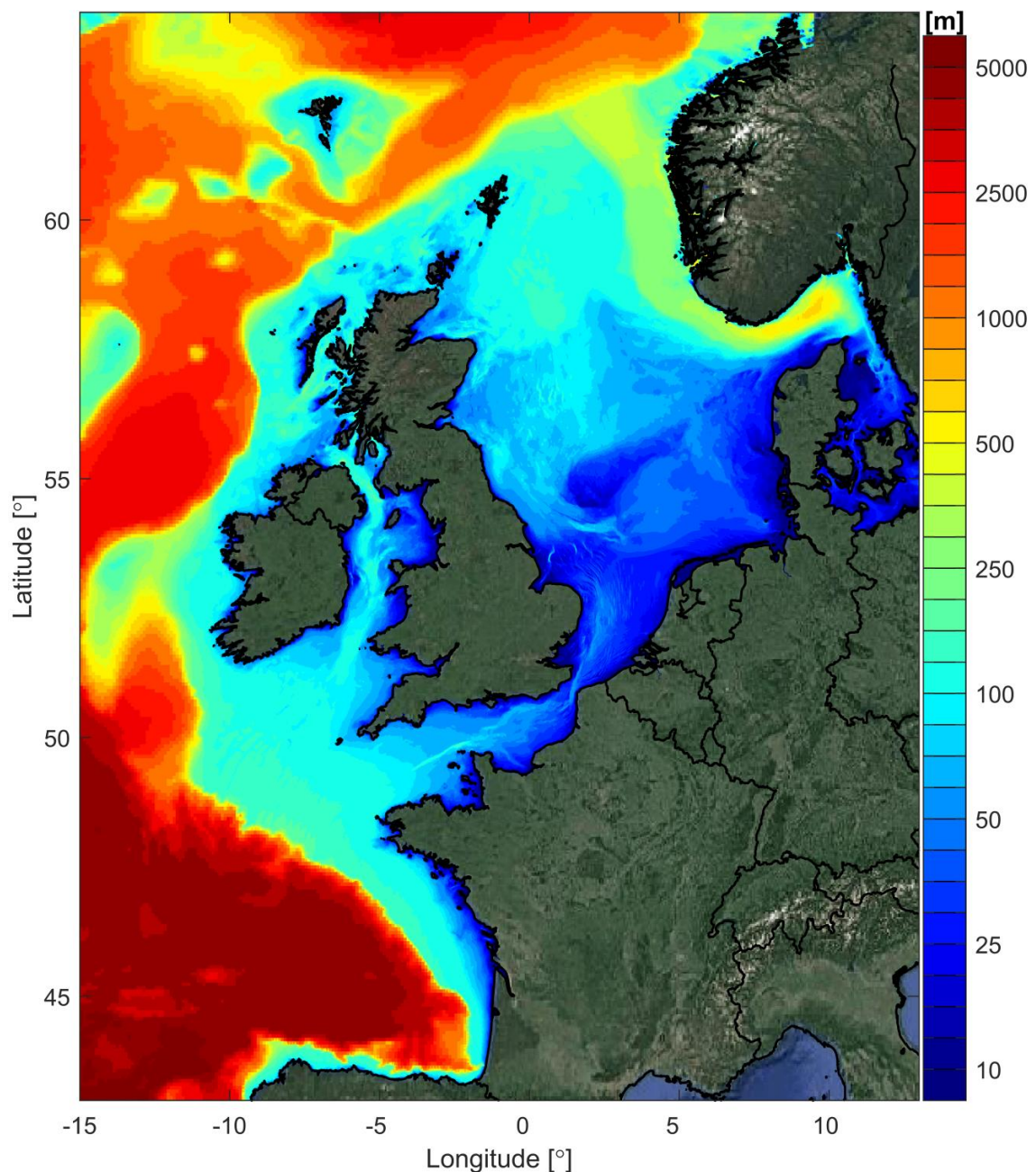


Figure 2.2 Overview of the DCSM-FM model bathymetry (depths relative to MSL).

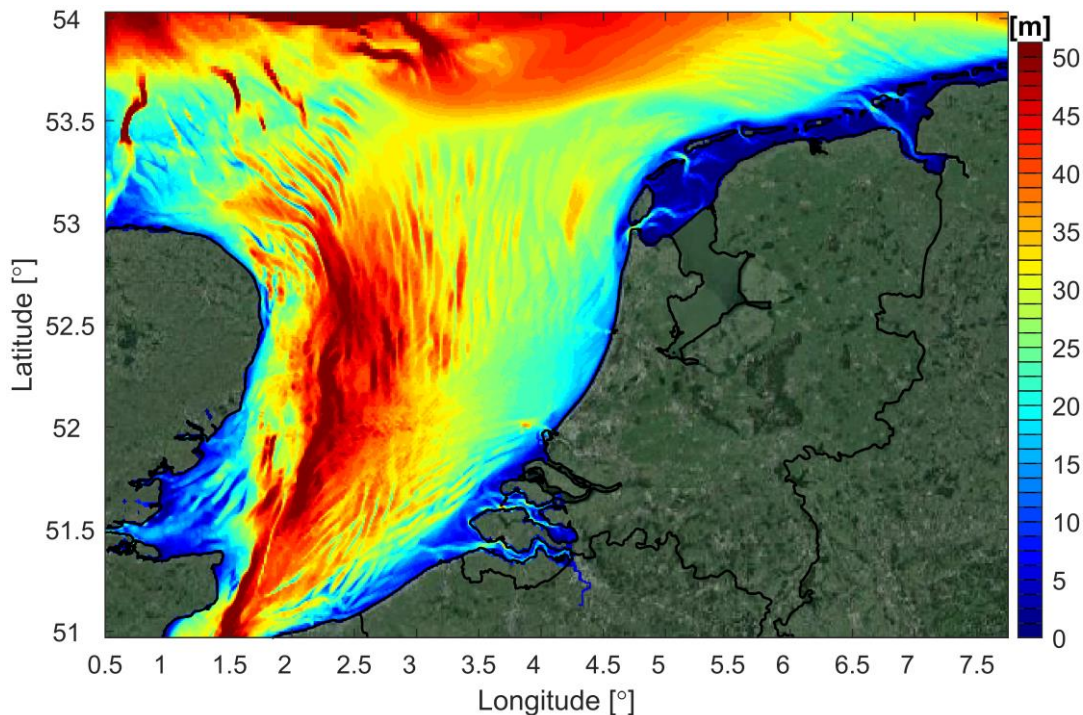


Figure 2.3 DCSM-FM model bathymetry in the southern North Sea (depths relative to MSL).

2.3 Bottom roughness

To account for the effect of bottom friction, a uniform Manning roughness coefficient of $0.028 \text{ s/m}^{1/3}$ was initially applied. During the (preliminary) model calibration this value was adjusted to obtain optimal water level representation. The minimum and maximum bottom roughness values applied are $0.014 \text{ s/m}^{1/3}$ and $0.0504 \text{ s/m}^{1/3}$.

2.4 Open boundary conditions

At the northern, western and southern sides of the model domain, open water level boundaries are defined. Water levels are specified at 209 different locations along those boundaries. In between these locations the imposed water levels are interpolated linearly.

Tide

The tidal water levels at the open boundaries are derived by harmonic expansion using the amplitudes and phases of 33 harmonic constituents. All except one were obtained from the global tide model FES2012, which provides amplitudes and phases of 32 constituents on a $1/16^\circ$ grid.

In addition, the solar annual constituent S_a has also been added. Even though in the ocean S_a is much less gravitational than meteorological and baroclinic in nature, in the absence of baroclinic forcing it is required to reproduce the observed residual annual cycle, i.e. the signal not captured by annual mean sea-level pressure and wind variations and notably the seasonal temperature cycle. While this is negligible on the shelf, this is less so in the deep ocean.

The above approach for S_a works reasonably well in the 2D barotropic model for which these boundary conditions have been derived. It is expected that in this 3D baroclinic version the

annual cycle will be overestimated, since variations in temperature and salinity are explicitly modelled. Removing the entire S_a signal from the open boundary forcing would probably not be sufficient to solve this, since the steric (i.e., due to changes in density) contribution to the water level variation on the open boundary is still missing.

Surge

While wind setup at the open boundary can safely be neglected because of the deep water locally (except near the shoreline), the (non-tidal) effect of local pressure will be significant. The impact of this is approximated by adding an Inverse Barometer Correction (IBC) to the tidal water levels prescribed at the open boundaries. This correction is a function of the time- and space-varying local air pressure.

Temperature and salinity

Temperature and salinity at the lateral open boundaries are derived from the World Ocean Atlas 2013 (WOA2013). This data set consists of climatological mean monthly fields on a 0.25° grid with 107 depth levels and vertical steps of 5 m at surface. These values are interpolated to the right horizontal location and 50 equally spaced depth levels (in sigma coordinates).

2.5 Meteorological forcing

2.5.1 Wind and pressure forcing

For meteorological surface forcing of the model time- and space-varying wind speed (at 10 m height) and air pressure (at MSL) are derived from the following sources:

- Hirlam7.2, with a spatial resolution of ~ 11 km and an hourly temporal interval (used for the simulations covering the period 2013-2017)
- ECMWF ERA-Interim (global atmospheric reanalysis), with a spatial resolution of approximately 80 km and a 3-hourly temporal interval (used for simulations covering the period 2006-2015)

The vertical distribution of the wind speed can be approximated with a logarithmic profile. Wind forcing of hydrodynamic models is commonly based on the meteorological standard height of 10 m above the surface (U_{10}). The wind stress at the surface, associated with the air-sea momentum flux, depends on the square of the local U_{10} wind speed and the wind drag coefficient, which is a measure of the surface roughness.

A Charnock formulation (with a non-dimensional Charnock coefficient) is used to link the sea surface roughness to the surface shear stress (Charnock, 1955). In the HiRLAM model a uniform, constant Charnock coefficient of 0.025 is assumed, which is also used in 3D DCSM-FM when this meteorological data source is applied. In ECMWF ERA-Interim, the Charnock coefficient is dependent on wind waves (as computed with the ECWMF WAM model) and consequently time and space dependent. When applicable, this is taken into account in the hydrodynamic model in a pre-processing step, through an adjustment of the U_{10} wind speed (i.e., with the use of pseudo-wind).

Relative wind effect

In most wind drag formulations the flow velocity is not taken into account in determining the wind shear stress (i.e., the water is assumed to be stagnant). Even though the assumption of a stagnant water surface is common because it makes computing stresses easier, from a physical perspective the use of relative wind speed makes more sense since all physical laws deal with relative changes. In case the flow of water is in opposite direction to the wind speed,

this would contribute to higher wind stresses (and vice-versa). The impact of the water velocity on the wind stress at the surface is taken into account in 3D DCSM-FM.

2.5.2 Heat-flux model and forcing

Spatial differences in water temperature, both horizontally and vertically, affect the transport of water through the impact it has on water density. Vertical temperature differences occur for example in the central North Sea, which is seasonally stratified due to heating of the water surface in summer. Furthermore, water temperature in shallow waters such as the Wadden Sea reacts faster to changes in meteorological conditions. This causes horizontal temperature gradients (and consequently density gradients) which under the right conditions can generate a surface flow towards deeper water and a bottom flow in opposite direction. To take these effects of temperature into account transport of temperature is modelled. An important driver is the exchange of heat with the atmosphere. Therefore, a surface heat flux model is used to compute the time-and space varying exchange of heat through the air-water interface. This model requires temporally varying data on air temperature at 2 m height, cloud cover, dew point temperature and wind speed. The incoming solar radiation is then computed by the heat flux model using the latitude on earth and the position of the earth relative to the sun based on the Julian day. The net solar radiation is computed by correcting for the cloud cover. The data sources for forcing the heat-flux model are the same as used for the wind forcing (cf. 2.5.1).

In the heat flux model used there are two proportionality coefficients that could be used as calibration parameters. These are the Stanton number for the convective (forced) heat flux and the Dalton number for the evaporative heat flux. In the present model a value (commonly found in literature) of $1.3 \cdot 10^{-3}$ is used for both the Stanton and Dalton number.

In the heat flux model, the Secchi depth is prescribed as a measure of the transparency of the water. The transparency of the water determines the distribution of incoming solar radiation over the water column. A constant, uniform Secchi depth of 4 m has been applied in the model settings.

2.6 River discharges

Fresh water discharges in the model domain are prescribed as climatological monthly means based on E-HYPE data for the years 1989-2013. This also holds for the water temperature associated with these discharges, while the salinity is set to a constant value of 0.001 psu, reflecting fresh water conditions. All discharges are prescribed in a depth averaged fashion.

Of the 895 E-HYPE based discharges imposed throughout the model domain, the six most important ones in the Netherlands are replaced by the following actual discharges as available in Waterbase:

- Den Oever Buiten
- Haringvlietsluizen Binnen
- IJmuiden Binnen
- Kornwerderzand Buiten
- Maassluis
- Schaar van Oude Doel

Since associated water temperatures are not available, these are set to a constant of 11 °C. The above discharges are not available for the year 2017. Therefore, climatological monthly means are used for that year, based on the data for the period 2007-2016.

2.7 Miscellaneous

2.7.1 Tidal potential

The tidal potential representing the direct body force of the gravitational attraction of the moon and sun on the mass of water has been switched on. It is estimated that the effect of TGF has an amplitude in the order of 10 cm throughout the model domain. Components of the tide with a Doodson number from 55.565 to 375.575 have been included.

2.7.2 Horizontal viscosity

The horizontal viscosity is computed with the Smagorinsky sub-grid model, with the coefficient set to 0.20. The use of a Smagorinsky model implies that the viscosity varies in time and space and is dependent on the local cell size. With the exception of a two nodes wide strip along the open boundaries no background value is specified. Along the open boundaries a value of 2000 m²/s has been used.

2.7.3 Initial conditions and spin-up period

At the start of the computations a uniform initial water level of zero elevation and stagnant flow conditions have been prescribed. The initial salinity is set to 35.1 psu, while the initial temperature is set to 5.5 °C, which is the average temperature along the open boundaries during the start of the computations. For spin-up from these conditions an entire calendar year is used.

2.7.4 Time zone

The time zone of DCSM-FM is GMT+0 hr. This means that the phases of the harmonic boundary conditions and the tidal potential are prescribed relative to GMT+0 hr. As a result, the output of DCSMv6 is in the same time zone.

2.7.5 Computational time

In Table 2.1 the computational time of DCSM-FM is presented together with the (average) time step and cell size and the number of network nodes. This is done for a number of configurations of the model, with all computations performed on Deltares' h6 cluster using 5 nodes with 4 cores each.

Table 2.1 Overview of grid cell size, number of net nodes, maximum and average numerical time step and computational time for various three-dimensional configurations of the model. The computations were performed on Deltares' h6 cluster using 5 nodes with 4 cores each.

Model	cell size (nm)	# layers	# nodes	Maximum time step (s)	Average time step (s)	Comp. time (min/day)	Comp. time (hr/year)
3D DCSM-FM (org)	4nm-1nm	25	353,314	200	191.1	5.7	35
3D DCSM-FM (1nm)	4nm-1nm	20	373,522	200	196.0	4.8	29
3D DCSM-FM (0.5nm)	4nm-0.5nm	20	629,187	120	111.2	13.0	79

3 Model validation: water levels

In Table 2.1, the quality of the water level representation of three configurations of the 3D DCSSM-FM model is presented for the calendar years 2013-2015 in terms of the Root-Mean-Square Error (RMSE). This is done for a selection of 13 stations along the Dutch coast, considering tide, surge, total water level. The tidal and surge part of the total water level were derived by mean of harmonic analysis using t_{tide} and prescribing a set of 118 constituents. The models were forced with Hirlam7.2 meteorological data. These results show an average total water level RMSE of 9-10 cm for all three configurations. Although differences are relatively small, the 0.5 nm version is slightly better than the 1 nm version, while the original configuration produces the best results in terms of total water levels. In all versions the contribution of the tide to the total water level error is larger than the contribution of the surge.

Note that these results are valid for Dutch coastal stations. In areas with larger variability in geometry and bathymetry (such as the Wadden Sea and Dutch estuaries) the beneficial impact of increased horizontal grid resolution is much larger. The fact that the original configuration performs slightly better is presumably because the calibration of the 2D schematization on which this model was originally based underwent a more thorough calibration in which the bathymetry was also used as a calibration parameter (cf. Zijl et al., 2013).

Table 3.1 Comparison of water level representation (RMSE, determined for the years 2013-2015) between three different version of 3D DCSSM-FM, at 13 locations along the Dutch coast, for tide, surge and total water level signal.

Station	RMSE tide (cm)			RMSE surge (cm)			RMSE water level (cm)		
	org	1nm	0.5nm	org	1nm	0.5nm	org	1nm	0.5nm
Cadzand	7.6	7.7	7.3	5.9	5.7	5.5	9.6	9.6	9.2
Westkapelle	8.5	8.4	8.3	5.6	5.5	5.4	10.2	10.0	9.9
Roompot Buiten	7.6	8.5	9.6	5.5	5.7	5.5	9.4	10.3	11.1
Brouwershavense G 8	7.2	7.0	6.9	6.5	6.4	6.4	9.5	9.4	9.2
Haringvliet 10	7.9	8.8	7.8	5.8	5.9	5.8	9.8	10.6	9.7
Hoek van Holland	6.3	11.7	9.9	6.2	6.7	6.4	8.8	13.4	11.8
Scheveningen	7.2	9.7	8.0	6.0	6.1	6.0	9.3	11.4	10.0
Ijmuiden Buitenhaven	7.2	10.2	7.8	6.0	6.3	6.1	9.3	12.0	9.9
Petten Zuid	6.8	9.8	9.0	7.1	7.3	7.3	9.8	12.2	11.6
Platform K13a	4.3	7.6	6.7	4.4	4.4	4.3	6.2	8.8	8.0
Terschelling Noordzee	3.9	7.0	6.4	5.8	5.6	5.6	7.0	9.0	8.5
Wierumergronden	6.4	6.8	6.3	5.6	5.3	5.3	8.5	8.7	8.2
Huibertgat	7.9	7.5	6.6	6.1	5.7	5.6	9.9	9.4	8.6
average	6.8	8.5	7.8	5.9	5.9	5.8	9.0	10.4	9.7
RMS	7.0	8.6	7.8	5.9	5.9	5.8	9.1	10.5	9.7

In Table 3.2 the skill of the 0.5 nm version of 3D DCSSM-FM is compared to a 2D barotropic version of the same model. These results show that especially the tide representation quality has reduced in the 3D version. This is further illustrated by the results in Figure 3.1, where the tidal component of the high water error (black dots) at tide gauge station Platform K13a is plotted for both the 2D and 3D version of the model. The main difference between both is the

occurrence of an error signal in the 3D results with a distinct annual periodicity. This is presumably caused by double counting in imposing the annual seasonal cycle S_a in the 3D model (cf. section 2.4).

Table 3.2 Comparison of the tide, surge and total water level representation (in 2013-2015), between a 2D and 3D version of DCSM-FM, quadratically averaged over 13 locations along the Dutch coast.

Station	RMSE tide (cm)	RMSE surge (cm)	RMSE water level (cm)
2D	5.9	5.6	8.1
3D	7.8	5.8	9.7

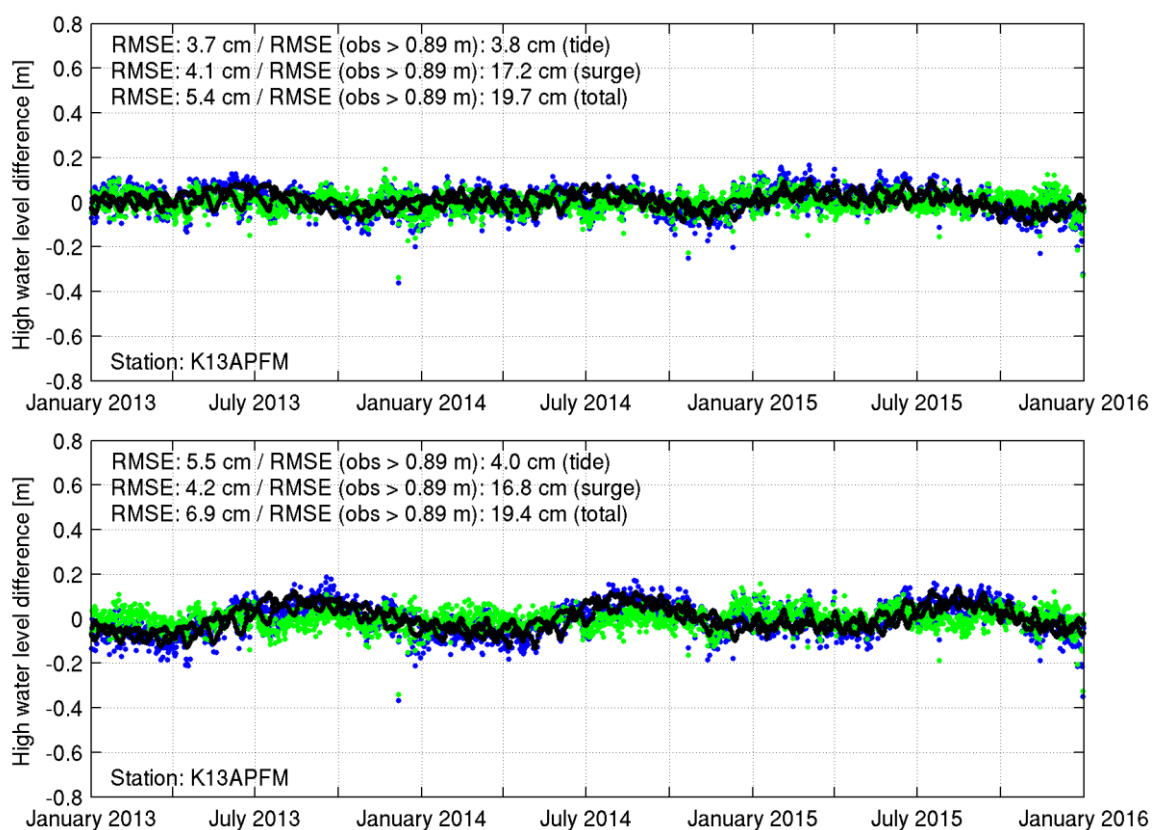


Figure 3.1 High water level error at tide gauge station Platform K13a for the period 2013-2015, for the 2D version (upper) and the 3D version (lower) of DCSM-FM (blue: total high water; black: tidal high water; green: skew surge).

Despite the deterioration of the tide representation in the 3D version of the model, 3D DCSM-FM still model performs substantially better than the official (3D) ZUNO-DD model (maintained by Rijkswaterstaat). This is demonstrated by the comparison for the year 2014 which is shown in Table 3.3, which shows that the model errors associated with the representation of tide, surge and total water level have decreased by more than 50%.

Table 3.3 Comparison of water level representation (RMSE, determined for 08-01-2014 to 01-01-2015) between ZUNO-DD and 3D DCSM-FM (0.5 nm), for tide, surge and total water level signal.

Station	RMSE tide (cm)			RMSE surge (cm)			RMSE water level (cm)		
	ZUNO-DD	0.5nm	%	ZUNO-DD	0.5nm	%	ZUNO-DD	0.5nm	%
Cadzand	30.5	7.5	-75%	13.1	5.4	-59%	33.2	9.2	-72%
Westkapelle	27.0	8.6	-68%	12.7	5.3	-58%	29.9	10.1	-66%
Haringvliet 10	21.1	8.0	-62%	11.9	5.6	-53%	24.3	9.8	-60%
Hoek van Holland	17.1	9.9	-42%	11.8	6.2	-47%	20.7	11.7	-43%
Scheveningen	19.5	8.0	-59%	12.0	5.8	-52%	22.9	9.9	-57%
Ijmuiden Buitenhaven	18.7	7.7	-59%	12.2	5.8	-52%	22.4	9.6	-57%
Average	22.3	8.3	-63%	12.3	5.7	-54%	25.6	10.1	-61%

4 Model validation: water temperature

4.1 Sea surface temperature

In this section computed sea surface temperature is compared to in-situ measurements for the seven-year period 2006 to 2012 at the locations shown in Figure 4.1. The three configurations of the model were forced with ECMWF ERA-Interim meteorology.

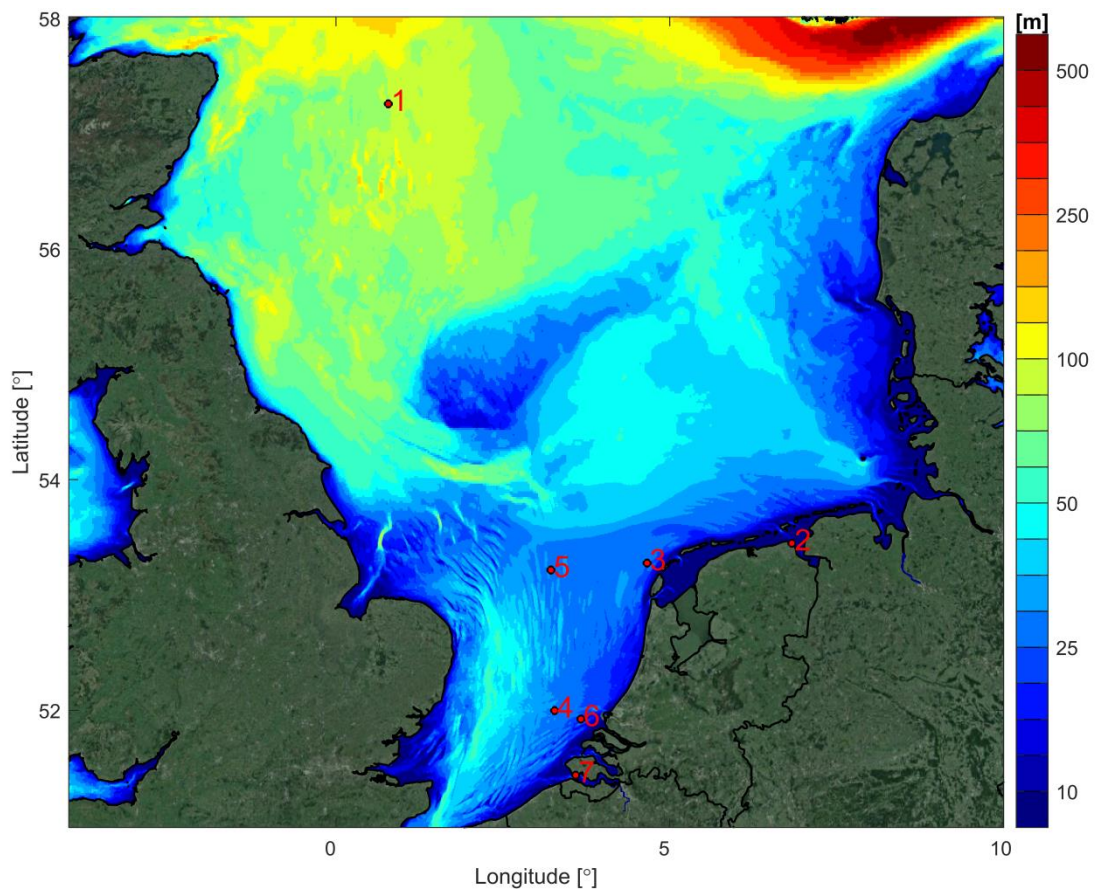


Figure 4.1 Locations of sea surface temperature measurements. The numbers refer to the station numbers in Table 4.1.

In Figure 4.2 to Figure 4.4, a selection of three computed sea surface temperature time series from the 0.5 nm version of the model are plotted together with the measured values. Based on this we conclude that there is a good representation of sea surface temperature. With respect to the temporal variation, the inter-annual variability is well represented. Also spatially the model is able to capture the variation in seasonal temperature amplitude with less variability offshore (Anasuria and Platform K13a) and more in coastal and estuarine location (e.g. Vlissingen). The quality of the temperature representation is also shown quantitatively in Table 4.1. These results show that while there is an average bias of 0.5 °C, the bias in Anasuria is double that. The results in Figure 4.4 show that this is mainly due to an underprediction of winter temperatures. Since the other stations don't exhibit this behaviour it might be expected that this is related to a poorer temperature representation in deeper water, possible due to a significantly larger vertical layer thickness in deep waters.

Table 4.1 Overview of the quality of the sea surface temperature representation in the 3D DCSM-FM model, in terms of bias, standard deviation (std) and Root-Mean-Square Error RMSE.

#	stationname	bias (°C)			std (°C)			RMSE (°C)		
		org	1nm	0.5nm	org	1nm	0.5nm	org	1nm	0.5nm
1	Anasuria	-1.03	-0.76	-0.76	0.65	0.65	0.61	1.22	1.00	0.97
3	Eierlandse Gat	-0.45	-0.38	-0.39	0.55	0.45	0.46	0.71	0.59	0.61
6	Europlatform	-0.23	-0.12	-0.15	0.53	0.39	0.42	0.58	0.41	0.45
5	Platform K13a	-0.51	-0.48	-0.48	0.45	0.45	0.44	0.68	0.66	0.65
4	Licheiland Goeree	-0.17	-0.16	-0.20	0.53	0.49	0.50	0.55	0.52	0.54
7	Vlissingen	-0.46	-0.41	-0.44	0.71	0.48	0.58	0.85	0.63	0.73
2	Eemshaven	-0.44	-0.27	-0.23	0.61	0.69	0.80	0.75	0.74	0.83
	average	-0.47	-0.37	-0.38	0.58	0.52	0.54	0.76	0.65	0.68

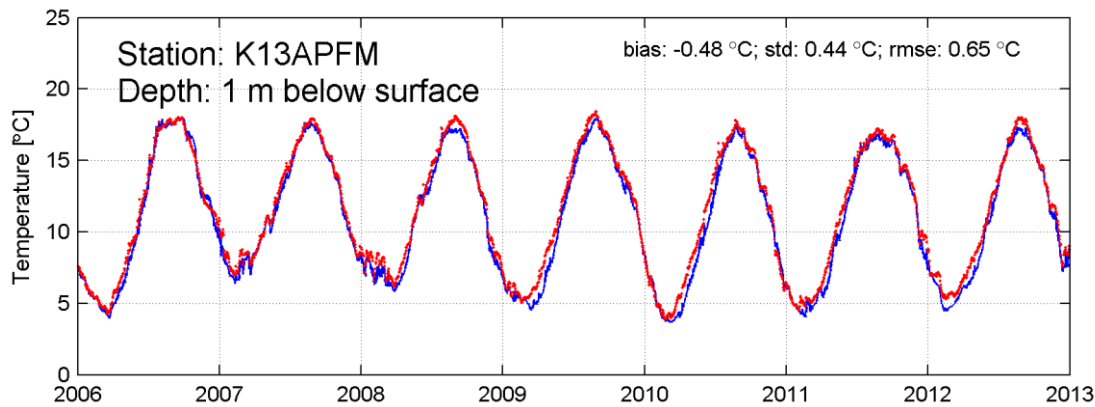


Figure 4.2 Time series of computed sea surface temperature (blue lines; 3D DCSM-FM 0.5 nm) for station Platform K13a together with measured values (red line).

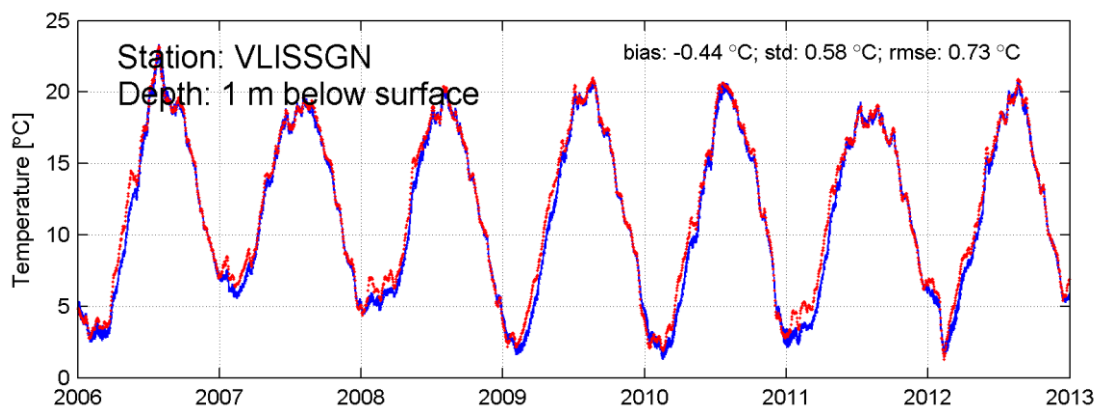


Figure 4.3 Time series of computed sea surface temperature (blue lines; 3D DCSM-FM 0.5 nm) for station Vlissingen together with measured values (red line).

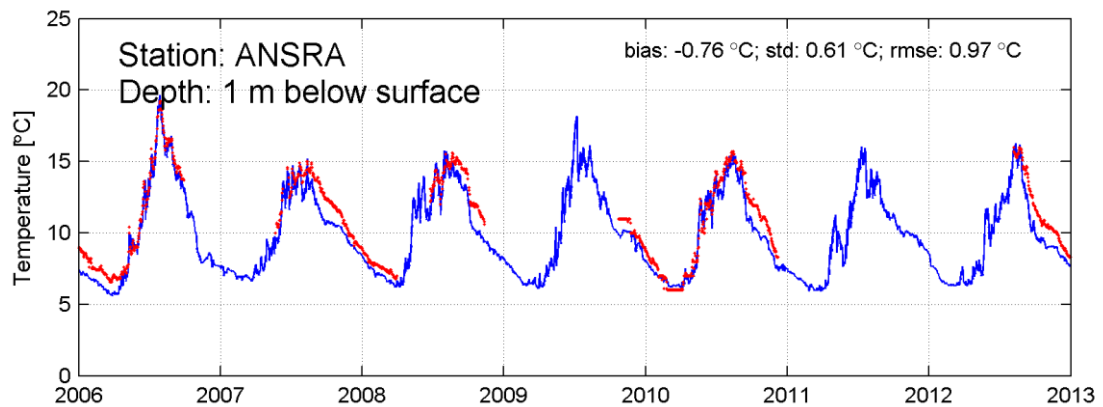


Figure 4.4 Time series of computed sea surface temperature (blue lines; 3D DCSM-FM 0.5 nm) for station Anasuria together with measured values (red line).

4.2 Temperature stratification in the central North Sea

Transport in the North Sea is affected by seasonal temperature stratification in the central North Sea. The relevance of this is illustrated with the fact that in the past, underprediction of the inter-annual variation of temperature stratification by ZUNO-DD was given as the main reason for explaining incorrect oxygen profiles in subsequent primary production simulations.

In Figure 4.5 the location of a station is indicated where both surface and bottom temperature are measured (at 1 m and 35 m below surface). In Figure 4.6 these are plotted as time series and compared with model results from the 0.5 nm version of 3D DCSM-FM. These results show that there is a good match with surface temperatures. At the bottom the rate of increase in spring temperatures is underestimated, which points to a lack of vertical mixing and an overestimation of temperature stratification. This is also shown in Figure 4.7 where the modelled and measured vertical temperature differences are plotted together. Nonetheless, this figure clearly shows that inter-annual variation in seasonal temperature stratification is well represented.

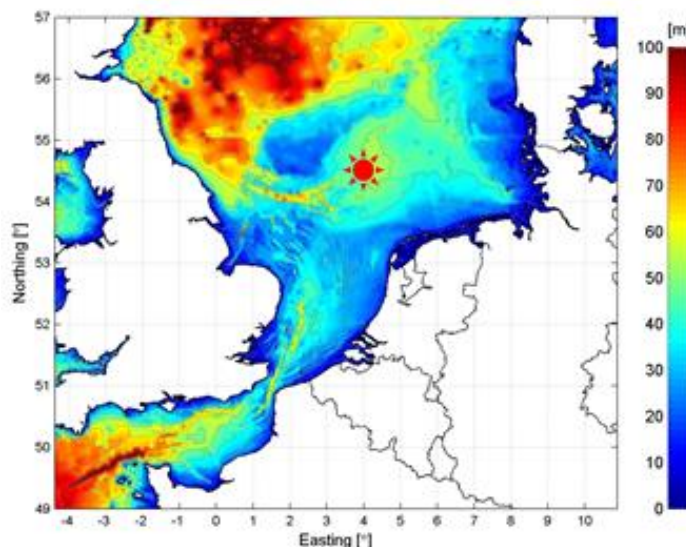


Figure 4.5 Location of station NL02, where water temperature is measured at 1 m and 35 m below the surface.

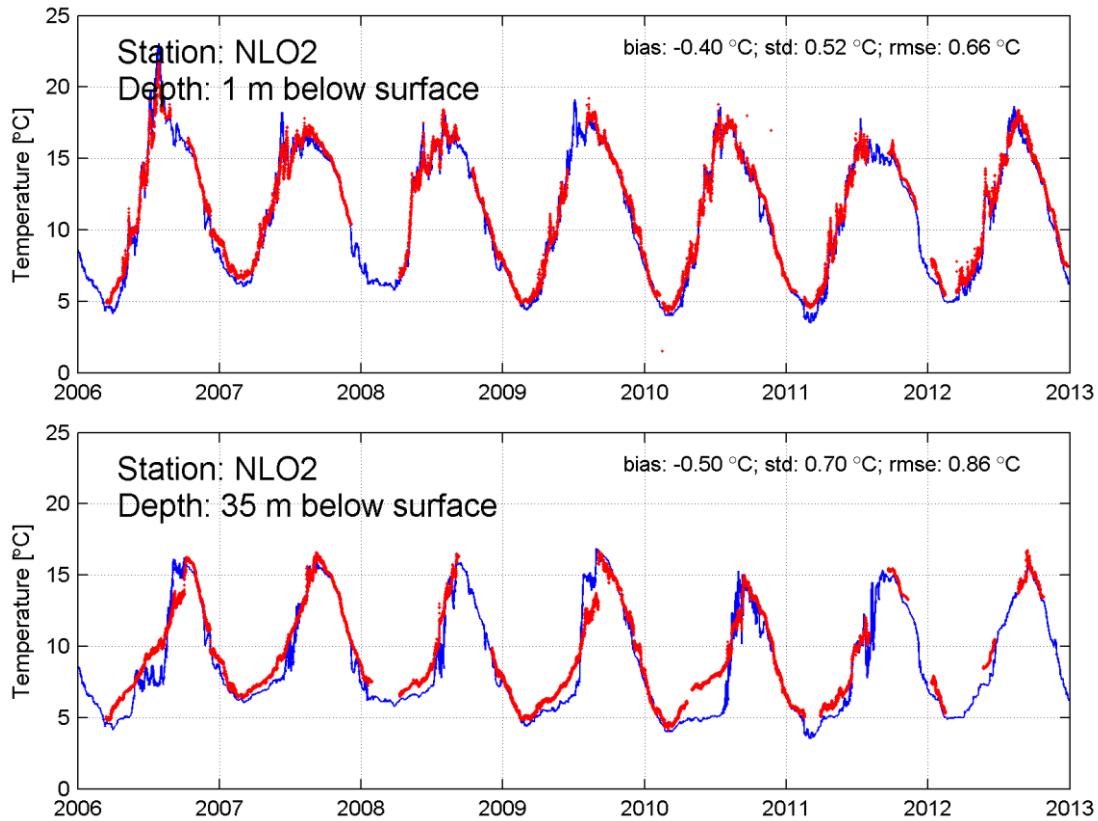


Figure 4.6 Time series of computed water temperature at 1 m (top) and 35 m (bottom) below surface (blue lines; 3D DCSM-FM 0.5 nm) at station NLO2 together with measured values (red lines).

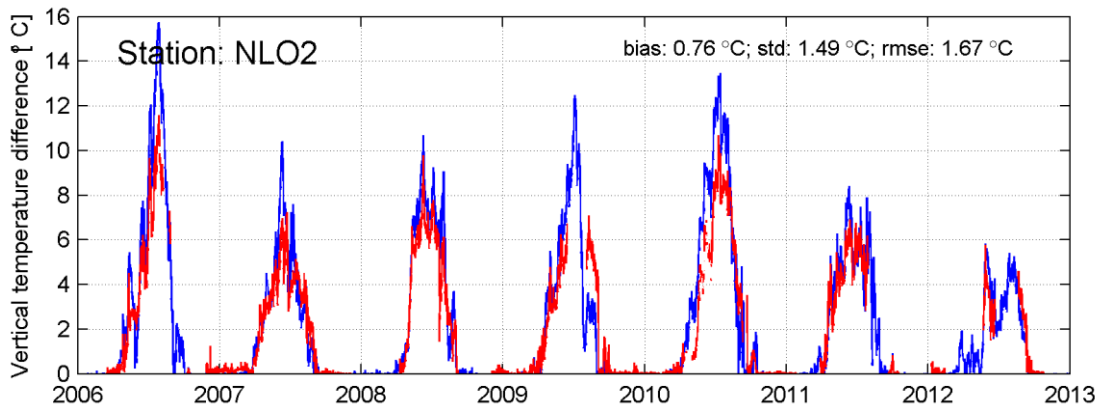


Figure 4.7 Time series of the vertical temperature difference (1m – 35 m below surface) at station NLO2 (blue: 3D DCSM-FM 0.5 nm; red: measurements).

In Table 4.2 the quality with which the temperature difference is represented in the model is further quantified for the three model versions. In deriving these statistics, vertical temperature differences of less than 0.5 °C have been ignored. These numbers show that all three versions on average overestimate temperature stratification, with the largest mean overestimation (0.76 °C) present in DCSM-FM 0.5 nm. Note that the 1 nm and 0.5 nm configuration differ also with respect the spatially varying bottom roughness applied. The comparison between modelled and measured temperature stratification is also shown visually as scatter plots for all three model configuration in Figure 4.8.

It should be noted that an overestimation is generally easier to improve than an underestimation. Assessing the sensitivity to the vertical background eddy diffusivity values is recommended and could lead to an improvement of the model.

Table 4.2 Quality of the representation of temperature stratification in the 3D DCSM-FM model, in terms of bias, standard deviation (std) and Root-Mean-Square Error RMSE.

	bias (°C)	std (°C)	RMSE (°C)
3D DCSM-FM (org)	0.32	1.01	1.06
3D DCSM-FM (1nm)	0.16	1.36	1.37
3D DCSM-FM (0.5nm)	0.76	1.49	1.67

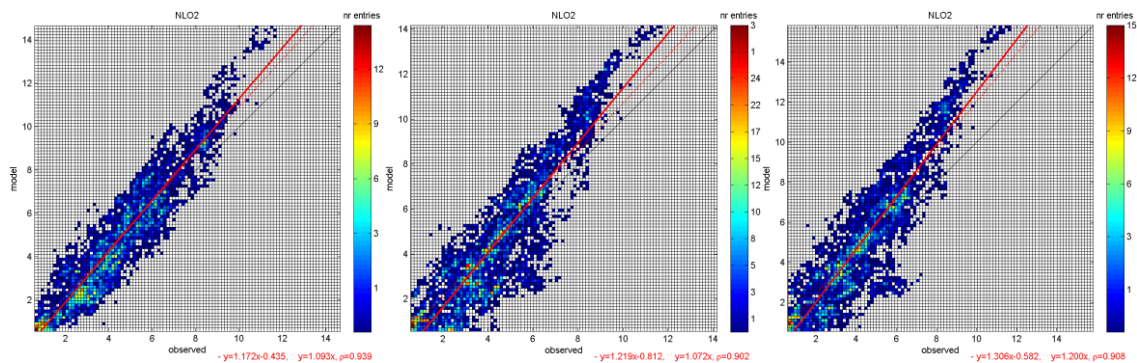


Figure 4.8 Scatter plots of observed and modelled temperature stratification in station NL02 (left: original configuration; middle: 1nm; right: 0.5 nm).

5 Model validation: sea surface salinity

In this section computed sea surface salinity is compared to measurements along two transects for the ten-year period 2006 to 2015. The three configurations of the model were forced with ECMWF ERA-Interim meteorology. Note that all river discharges in the original configuration are prescribed as monthly mean values (based on E-HYPE), while in the other configurations the RWS-provided actual discharges are used for the main Dutch discharges.

A quantitative assessment of the sea surface salinity representation is presented in Table 5.1 for the Noordwijk transect and in Table 5.2 for the Terschelling transect. These results show that the original configuration yields salinities that are generally lower than the other two configurations. The impact of resolution is limited at the Terschelling transect, while at the Noordwijk transect the bias decreases from 0.9 psu to 0.6 psu by an increase in resolution to 0.5 nm.

Table 5.1 Overview of the quality of the sea surface salinity representation in the 3D DCSM-FM model at the Noordwijk transect, in terms of bias, standard deviation (std) and Root-Mean-Square Error RMSE.

Station	bias (psu)			std (psu)			RMSE (psu)		
	org	1nm	0.5nm	org	1nm	0.5nm	org	1nm	0.5nm
Noordwijk 2 km	-0.6	1.4	0.9	1.7	1.4	1.4	1.8	2.0	1.6
Noordwijk 10 km	-0.9	0.8	0.5	1.4	1.2	1.2	1.7	1.4	1.2
Noordwijk 20 km	-0.5	1.3	0.8	1.4	1.2	1.2	1.5	1.8	1.4
Noordwijk 70 km	-0.2	0.2	0.2	0.3	0.3	0.3	0.3	0.3	0.4
average	-0.5	0.9	0.6	1.2	1.0	1.0	1.3	1.4	1.2

Table 5.2 Overview of the quality of the sea surface salinity representation in the 3D DCSM-FM model at the Terschelling transect, in terms of bias, standard deviation (std) and Root-Mean-Square Error RMSE.

Station	bias (psu)			std (psu)			RMSE (psu)		
	org	1nm	0.5nm	org	1nm	0.5nm	org	1nm	0.5nm
Terschelling 4 km	0.1	0.4	0.5	1.1	1.0	1.2	1.1	1.1	1.3
Terschelling 10 km	-0.2	0.5	0.6	1.0	0.8	0.8	1.0	1.0	1.0
Terschelling 50 km	0.2	0.7	0.6	0.5	0.5	0.5	0.5	0.9	0.8
Terschelling 100 km	0.3	0.6	0.6	0.2	0.2	0.3	0.4	0.6	0.6
Terschelling 135 km	0.4	0.6	0.6	0.3	0.3	0.3	0.5	0.7	0.6
Terschelling 175 km	0.3	0.5	0.4	0.2	0.3	0.2	0.4	0.5	0.5
Terschelling 235 km	0.1	0.3	0.3	0.2	0.3	0.3	0.3	0.4	0.4
average	0.2	0.5	0.5	0.5	0.5	0.5	0.6	0.7	0.8

Further inspection of the model results shows that the simulation with increased horizontal resolution exhibits more temporal variation in salinity. This is illustrated with the time series plot in Figure 5.1. The increased temporal variability is probably related to the finer spatial scales that can be resolved on a higher resolution grid. The impact on spatial sea surface salinity patterns is shown in Figure 5.2 and Figure 5.3, as snapshots for two moments in time.

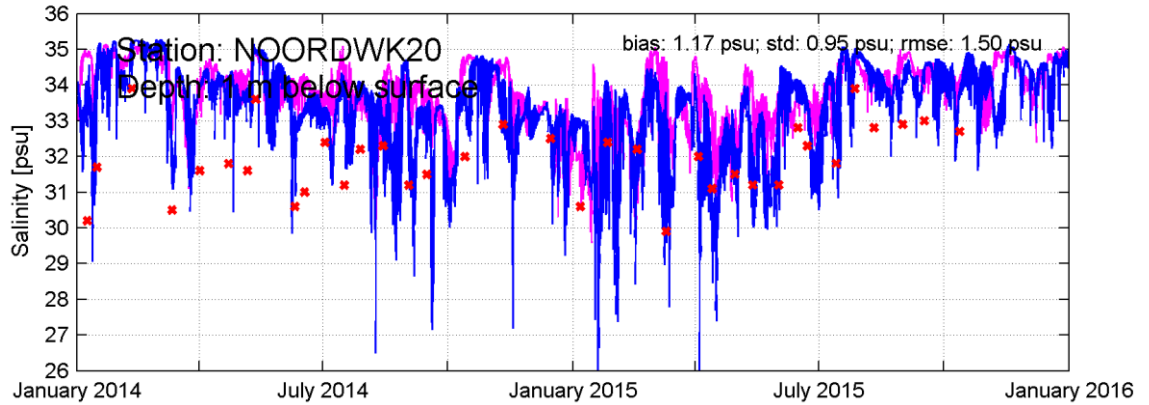


Figure 5.1 Sea surface salinity at location Noordwijk20 (20 km offshore) for the years 2014-2015 (red crosses: measurements; blue line: 3D DCSM-FM 0.5 nm; magenta line: 3D DCSM-FM 1 nm).

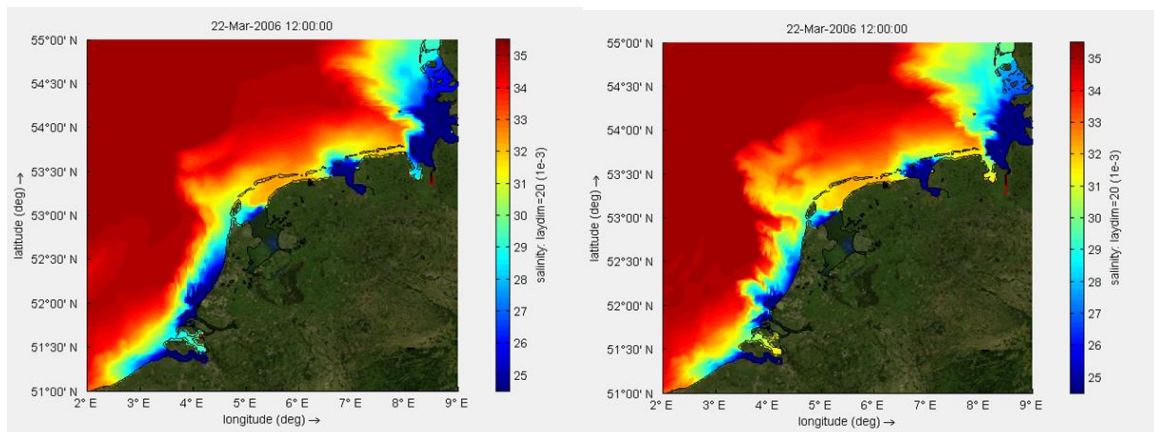


Figure 5.2 Sea surface salinity on 22-03-2006 as computed with the 1 nm (left) and 0.5 nm (right) version of 3D DCSM-FM.

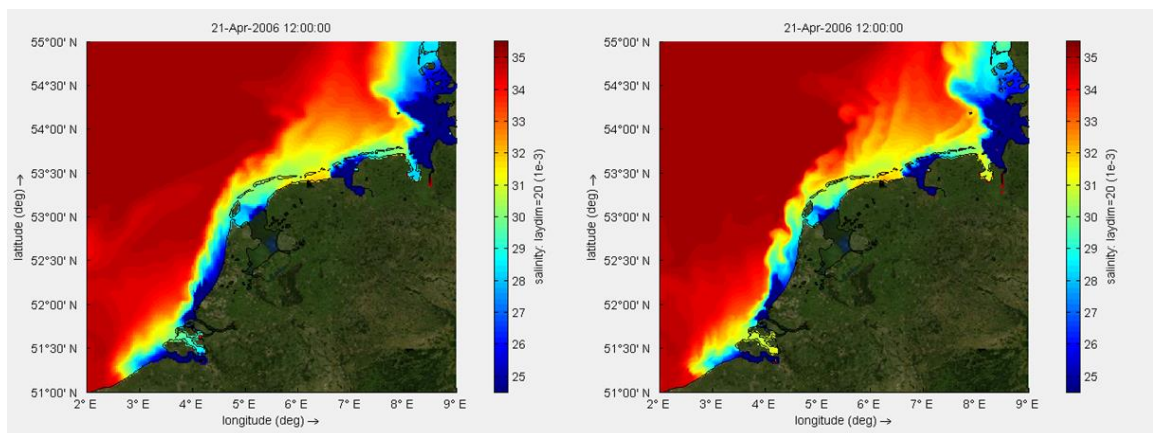


Figure 5.3 Sea surface salinity on 21-04-2006 as computed with the 1 nm (left) and 0.5 nm (right) version of 3D DCSM-FM.

The salinity in the Rhine ROFI is much more variable than the interval with which measurements are available. Therefore, it is also worthwhile to look at the computed mean cross shore salinity gradient compared to measurements. This is done in Figure 5.4 for the

Noordwijk transect and Figure 5.5 for the Terschelling transect. These figures show that the cross shore gradient is more or less well represented, with the original setup having a gradient that is somewhat too steep and the other two configurations showing less fresh water nearshore. Possible explanations for deviations from measured values are uncertainty in the discharge rate of the main rivers, or inaccuracies in the residual transport along the Dutch coast.

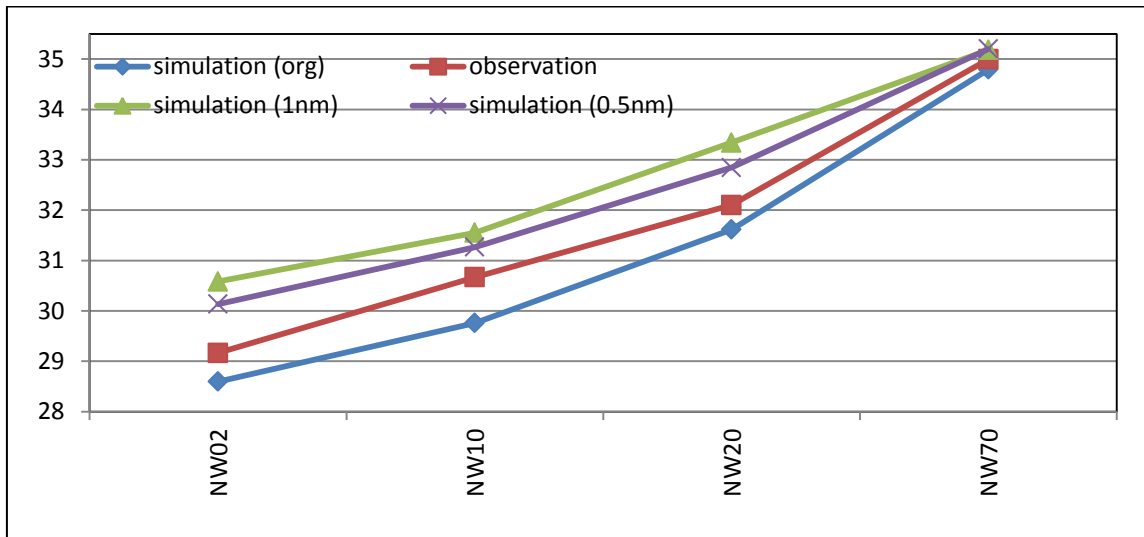


Figure 5.4 Mean observed and simulated salinity along the Noordwijk transect for the years 2006-2015.

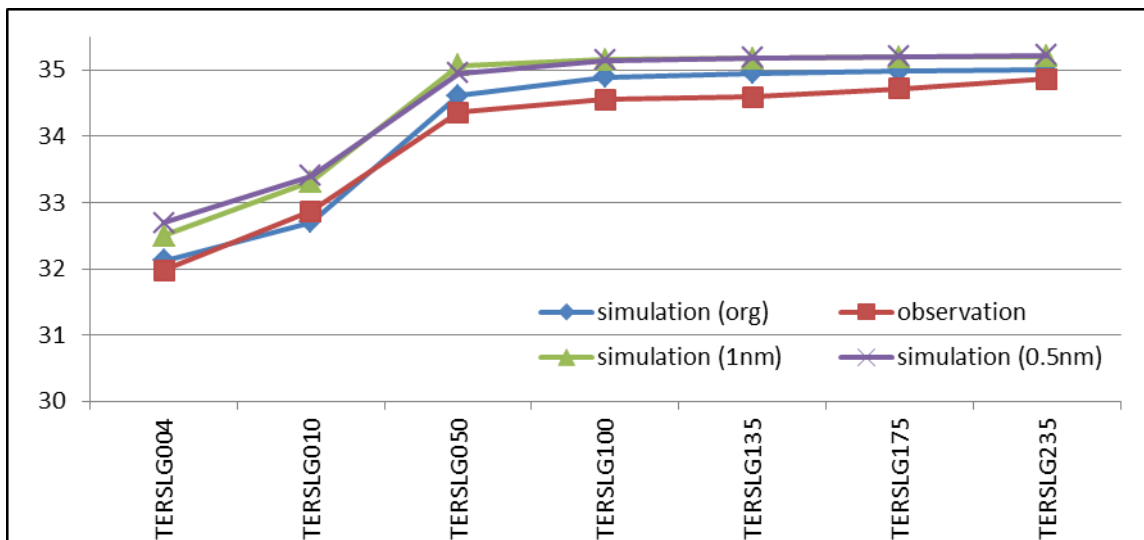


Figure 5.5 Mean observed and simulated salinity along the Terschelling transect for the years 2006-2015.

6 Residual transport through the English Channel

An important indicator of residual transport in the North Sea is the residual transport through the English Channel. It is commonly thought that the actual mean residual transport should be more than around $100 \cdot 10^3 \text{ m}^3/\text{s}$ (see Table 6.1). In past computations with the ZUNO-DD model this was achieved by tilting the southern boundary. Without tilting the residual transport was considered too low. In 3D DCSM-FM tilting the boundaries is impractical because the open boundaries are located much further away and the fact that there is no separate English Channel boundary.

Source	Year	Method	Tidal	Wind	Other	Total
Carruthers (1928)	1926-1934	(I)	-	-	-	164
Van Veen (1938)	1934-1936	(I)	-	-	-	112.5
Cartwright (1961)	1957-1958	(II)	50	-	-	235
Prandle and Harrison (1975)	1973	(II)	-	-	-	129
Alcock and Cartwright (1977)	1955-1965	(II)	-	-	-	168
Prandle (1978a)	1978	(IV)	82	37	41	160
Prandle (1984)	1951-1975	(IV)	50	-	-	90
Prandle (1993)	1990	(III)	36	45	6	87
Salomon and Breton (1993)	1983-1991	(IV)	37	-	-	114
Prandle et al. (1996)	1990-1991	(III)	41	47	6	94

Table 6.1 Residual flows based on historical measurements and numerical modelling. Flows are given in $10^3 \text{ m}^3 \text{ s}^{-1}$. Data obtained from (I) in situ measurements, (II) cable measurements (III) HFR & ADCP and (IV) model simulations. Table taken from (Van der Linden, 2014).

The residual transport through the English Channel is determined with for the 10-year period 2006-20115 for three configurations of 3D DCSM-FM. The results are presented in Figure 6.1 and show that there is considerable inter-annual variation in residual transport, ranging from $70 \cdot 10^3 \text{ m}^3/\text{s}$ to $180 \cdot 10^3 \text{ m}^3/\text{s}$ in the 0.5 nm version. Furthermore, in the original configuration the mean transport ($97 \cdot 10^3 \text{ m}^3/\text{s}$) is around the value minimally required, without the need to artificially adjust the open boundaries. On average the 1 nm and 0.5 nm configuration yield residual transports that are ~20% larger than the original configuration. This could be caused by a difference in Sa barotropic forcing on the open boundary (excluded in the original version, included in the other two version). The resolution (0.5 nm vs 1nm) has limited impact, except in the first years considered.

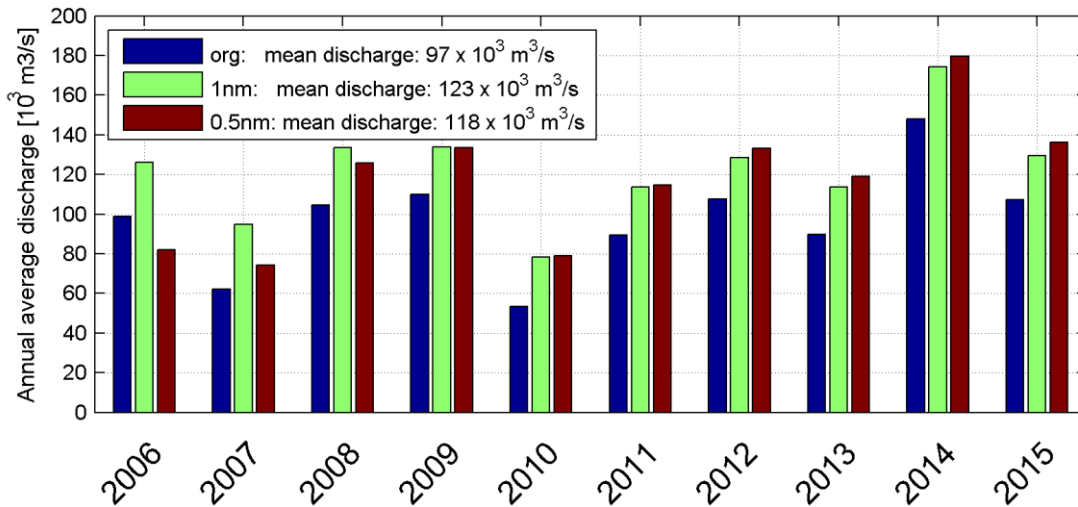


Figure 6.1 Annual average discharge through the English Channel computed with three different configurations of 3D-DCSM-FM.

In Figure 6.2 the impact of baroclinic (density-driven) phenomena on the residual transport is quantified. This shows that the residual transport is mostly caused by barotropic phenomena. Adding salinity and temperature in the 3D configuration adds a further 10-15%.

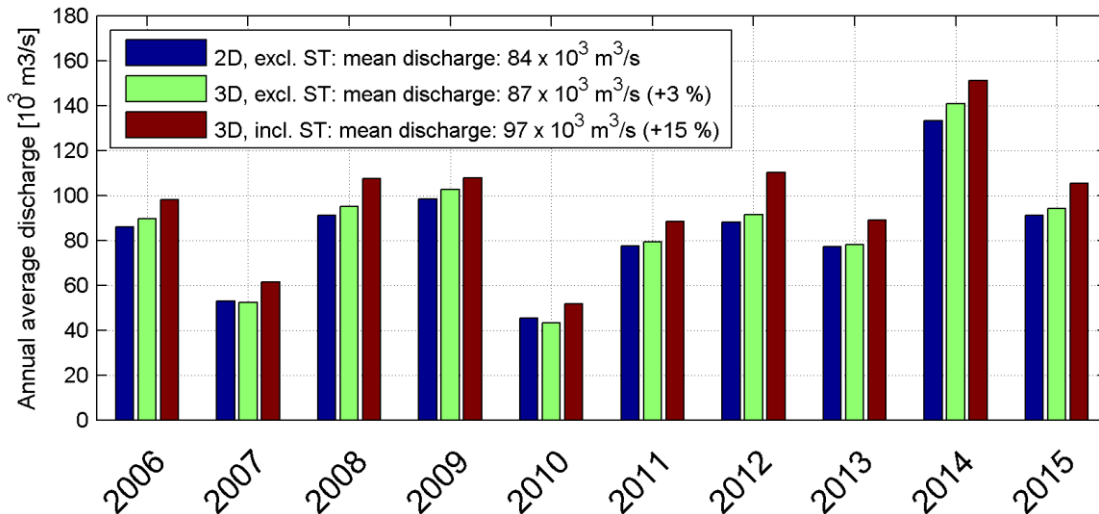


Figure 6.2 Annual average discharge through the English Channel computed with the original configuration of 3D-DCSM-FM (red), a 3D configuration with uniform density (salinity and temperature) and a 2D configuration with uniform density.

7 Comparison with observed flow velocities

7.1 Introduction

In order to compare the current velocities of the models and measurements, a distinction is made between the magnitude and direction. The time series of both parameters are compared visually and statistically (correlation coefficient r , bias, standard deviation and RMSE).

Furthermore, the variation of the model quality over the vertical is assessed by comparing the accuracy for the depth averaged values as well as several locations in the water column and vertical velocity profiles. In case of the specific layers, the model layer closest to the measurement point is chosen. The comparison between the different model resolutions and the variation of quality over the vertical is done through a table with statistics.

7.1 Data availability

Several sources of data with respect to current measurements are available. Table 7.1 provides an overview, including the location, approximate depth, vertical extent, period and duration.

Table 7.1 Overview of flow velocity measurement campaigns and sources

Campaign/source	Location, offshore	Vertical extent	Period, duration
Building with Nature	Wijk aan Zee, Egmond, Camperduin 0.25-7 km offshore	Every 0.5 meter starting at 2m from water surface	Separate days in 2010/2011. 1-2 hour time step due to sailing measurements
LaMER	Egmond, 9-11 m depth	0.3 m above bed	4x >2 week in 2010. 10 minute time step.
Nourtec	Terschelling, 1700m from shoreline	0.25 m above bed	May/June 1994, Oct/Nov 1994, Oct/Nov 1995. 1 hour time step with missing values.
Zeeuwse data, W7 buoy	Kruishoofd (Western Scheldt estuary mouth), 1700 m from shoreline		Jul/Aug 2007 and Aug/Sep/Oct 2008. 10 minute time step.
FINO buoy	43 km from Wadden Islands	From 2 to 30 meter, with steps of 2 meter	Ongoing, 60 minute time step
Matroos	Eems, IJ and New Waterway estuary mouths	Varying, often 1 point in water column	Ongoing, 10 minute time step
STRAINS	2 and 6 km from the shore of	From 0.8 m above bed, every 0.5 m up	23 Feb to 7 Mar 2013 and 15 Sep to 28 Oct

	Kijkduin/Zandmotor (12 and 18 m depth)	to the water surface	2014
Sandpit	2.2 and 10.5 km from the shore of Noordwijk (15 and 18 m depth)		2003
Monopiles HKZ A/B	27 and 28 km from the shore of Scheveningen (23 and 24 m depth)	From 4 to 20 m below the water surface, with an interval of 2 m	June 2016 to December 2017, 10 minute time step
Monopiles HKN A/B	27 km from the shore of Egmond	From 4 to 20 m below the water surface, with an interval of 2 m	April to Sep 2017, 10 minute time step
Kustgenese Ameland	1.7 – 7 km from the shore of Ameland (10 to 16 m water depth)	From 3-4 meter above the bed up to the water surface, with an interval of 0.8 m	(Sep/Oct/Nov/Dec 2017, 2-4 weeks per measurement frame, 10 minute time step
Kustgenese Terschelling	4.7 – 7 km from the shore of Terschelling		

7.1.1 Selected data

A selection of the available data is used to validate the 3D DCSM-FM model:

- Monopiles HKZ A/B
- Kustgenese measurements near Ameland

In choosing these data for validation, several considerations played a role. For instance, offshore data is preferred above estuary measurements. Finally, it is preferred to validate with data in the same period of time in order to keep the model output manageable.

HKZ A/B

The data from the two buoys deployed by Fugro (HKZA_WS149 and HKZB_WS158) are located 27 to 28 km offshore from the Egmond coast (see Figure 7.1), where the water depth is approximately 23 m. Both buoys collected velocity data at 9 vertical locations, between 4 m and 20 m below the water surface, with an interval of 2 meters. The data collection started in June 2016, but the data from HKZA_WS149 is only available from November 2016. The data is available until December 2017.

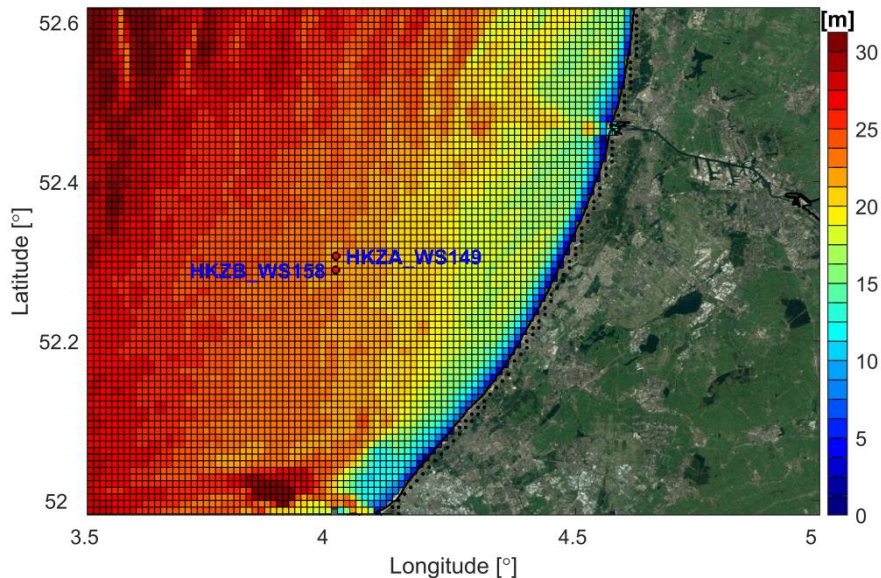


Figure 7.1 Location of the HKZA and HKZB measurement buoys.

Kustgenese 2 measurements near Ameland

The data from the Kustgenese 2 campaign is measured from measurement frames located on the bed in 11 m to 20 m of water depth (see Figure 7.2). The current velocity data is collected with ADCP instruments, measuring from 3 m to 4 m from the bed towards the water surface, with an interval of 0.8 m. The measurement frames collected in different periods of 2 to 4 weeks in November and December 2017. Note that since the ADCP data has not been corrected for deviations of the compass, it is possible that there is a 5-15 degree deviation from the actual current direction.

In addition, Aquadop measurements have also been performed, which contain the velocities near the bottom. However, since these are not yet available they have not been used in the present analysis.

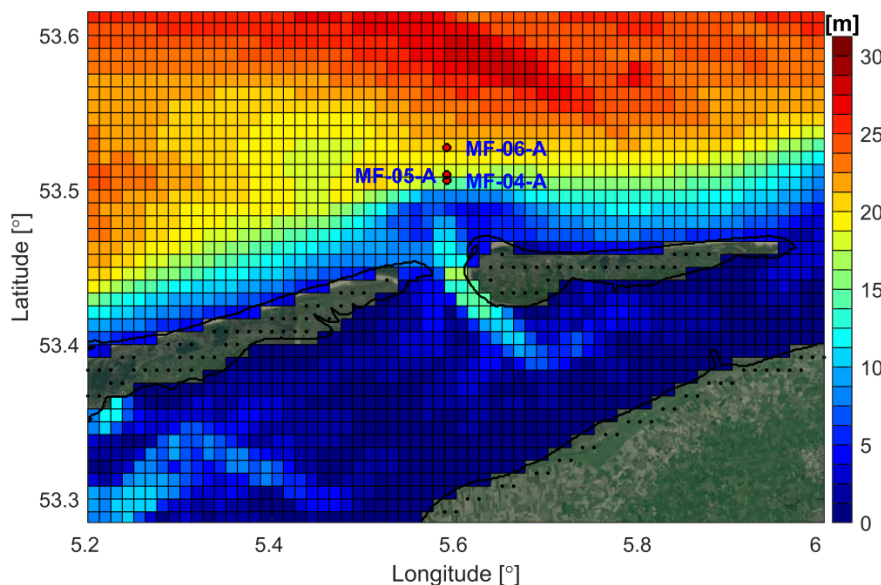


Figure 7.2 Location of the Kustgenese 2 measurement frames near Ameland with in the background the network and bathymetry of 3D DCSM-FM 0.5 nm.

7.2 HKZ A/B

7.2.1 Visual comparison

Figure 7.3 and Figure 7.4 show time series and scatter plots of the model (0.5 nm and 1 nm, respectively) and measurements for an arbitrary two-week period. In these figures the velocity vector is split in a magnitude and the direction. Current directions for velocity magnitudes lower than 0.2 m/s are ignored in all plots and subsequent analysis.

These figures show that the model accurately reproduces the timing of the peak velocities and slightly overestimates the magnitudes. The latter is also apparent from the velocity magnitude scatter plots, which have most dark colours (representing higher point density) as well as the linear regression line (blue line) above the diagonal (dashed line). The overestimation of the magnitude is visible over the entire period where the model is compared to the measurements.

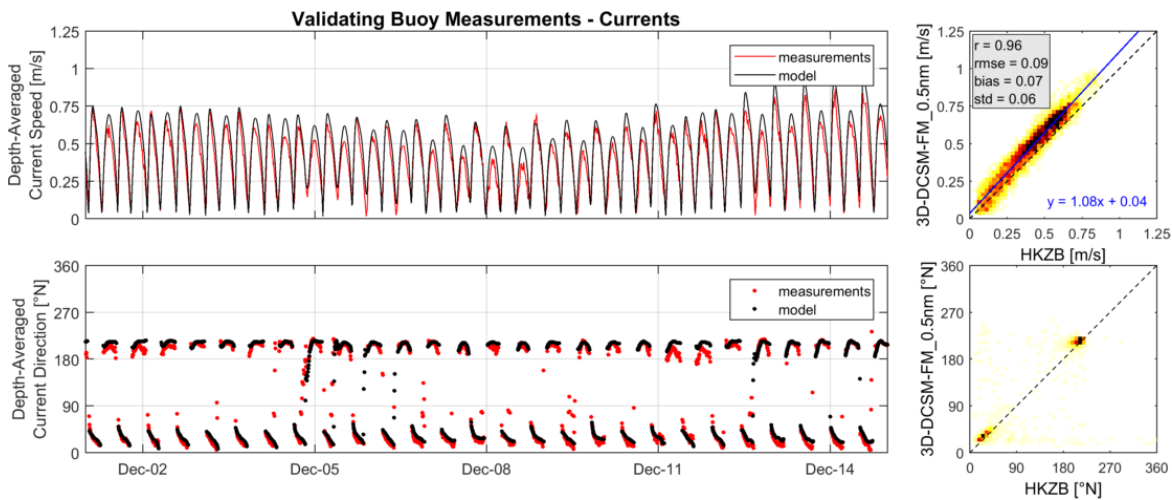


Figure 7.3 Time series and statistics of the comparison with the depth averaged values of the 0.5nm 3D model for station HKZB_WS158 and for the first two weeks of December 2016.

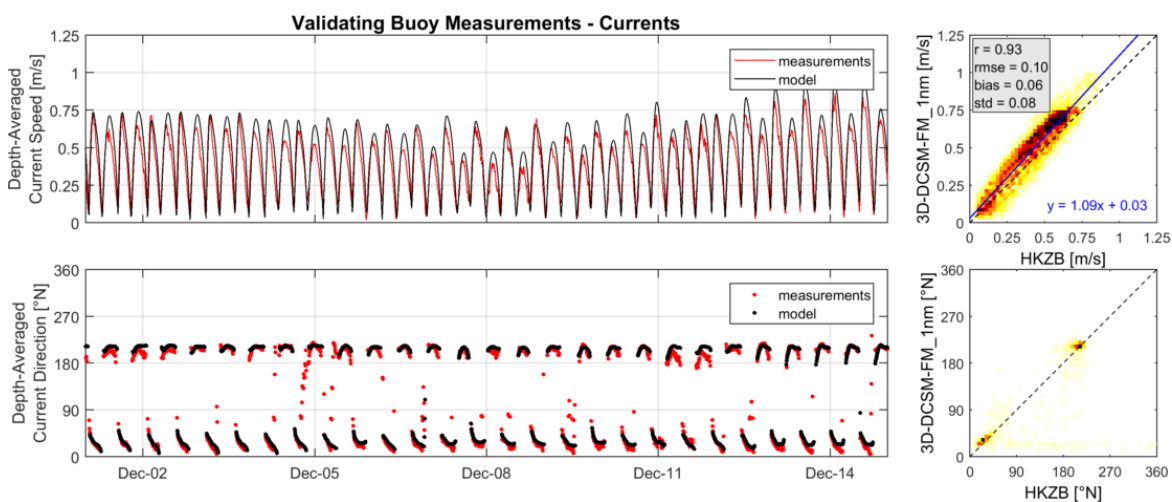


Figure 7.4 Time series and statistics of the comparison with the depth averaged values of the 1nm 3D model for station HKZB_WS158 and for the first two weeks of December 2016.

7.2.2 Quantitative comparison

In order to quantitatively compare the results for the different model configurations, measurement locations and vertical positions, all statistics are summarized in Table 7.2. The accompanying scatter plots for station HKZB are presented in Figure 7.5 to Figure 7.8. The results in this table and these figures represent the comparison for the period for which measurements are available in the years 2016 and 2017. For HKZB this covers June 2016 to December 2017, whereas for HKZA November 2016 to December 2017 are covered.

The results in the table make clear that all three configurations of the model overestimate the velocity magnitude (indicated with positive values for the bias). In HKZB the depth-averaged current velocity is overestimated by 6-7 cm/s, while in HKZA this is 2-3 cm/s (depending on the model configuration).

Impact of resolution

The standard deviation of the magnitude error is generally lowest for the 0.5 nm configuration (depth averaged: 6 cm/s for HKZA and HKZB) and highest for the original configuration (depth averaged: 9 cm/s for HKZA and HKZB). This also holds for the correlation coefficient and implies that the current representation improves by increasing the model resolution from 1 nm ($R=0.89$) to 0.5 nm ($R=0.95$). This is apparent for all depths and both HKZ stations and can also be seen visually by comparing Figure 7.3 and Figure 7.4, in which only the model resolution differs. Generally, the width of the scatter is narrower for the 0.5 nm model configuration.

Table 7.2 Summary of the statistics of the data-model comparison for stations HKZA (November 2016 to December 2017) and HKZB (June 2016 to December 2017).

Model		0.5 nm				1 nm				org				
		DA	4m	12m	20m	DA	4m	12m	20m	DA	4m	12m	20m	
HKZA	Depth [m]													
	magnitude	R [-]	0.95	0.89	0.95	0.88	0.92	0.84	0.92	0.83	0.89	0.81	0.89	0.81
	RMSE [m/s]	0.09	0.16	0.08	0.13	0.11	0.17	0.11	0.16	0.11	0.16	0.09	0.12	
	bias [m/s]	0.06	0.11	0.05	0.10	0.07	0.10	0.06	0.12	0.06	0.07	0.02	0.08	
	std [m/s]	0.06	0.12	0.07	0.08	0.08	0.14	0.09	0.10	0.09	0.14	0.09	0.09	
HKZB	magnitude	R [-]	0.96	0.90	0.95	0.85	0.93	0.87	0.93	0.81	0.89	0.83	0.90	0.79
	RMSE [m/s]	0.08	0.13	0.08	0.16	0.10	0.14	0.10	0.18	0.10	0.14	0.09	0.14	
	bias [m/s]	0.06	0.06	0.04	0.13	0.07	0.06	0.05	0.15	0.05	0.02	0.02	0.10	
	std [m/s]	0.06	0.11	0.07	0.09	0.08	0.13	0.08	0.11	0.09	0.14	0.09	0.09	

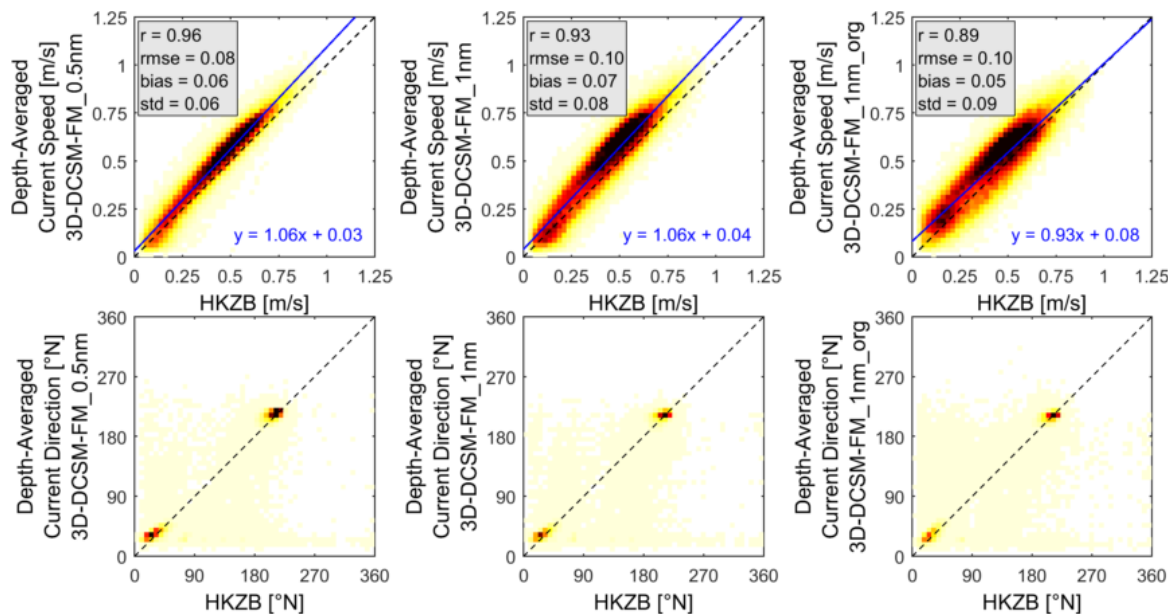


Figure 7.5 Scatter plots of **depth-averaged** current magnitude and direction at station HKZB_WS158 for the period June 2016 to December 2017 (left: 0.5 nm; middle: 1 nm; right: original).

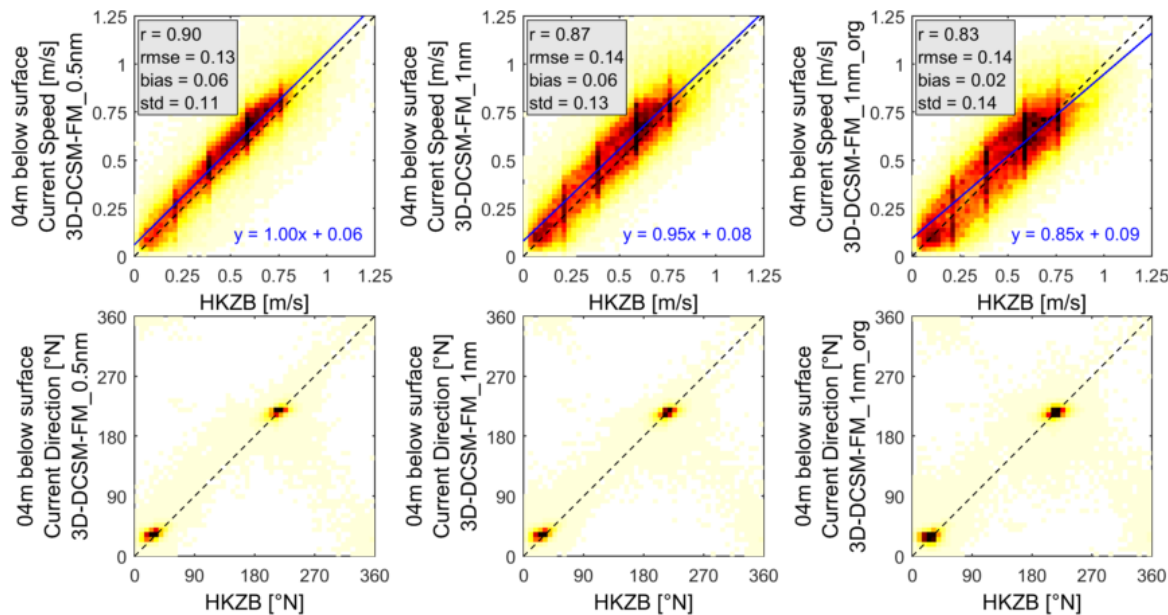


Figure 7.6 Scatter plots of current magnitude and direction at **4 m below the surface** at station HKZB_WS158 for the period June 2016 to December 2017 (left: 0.5 nm; middle: 1 nm; right: original).

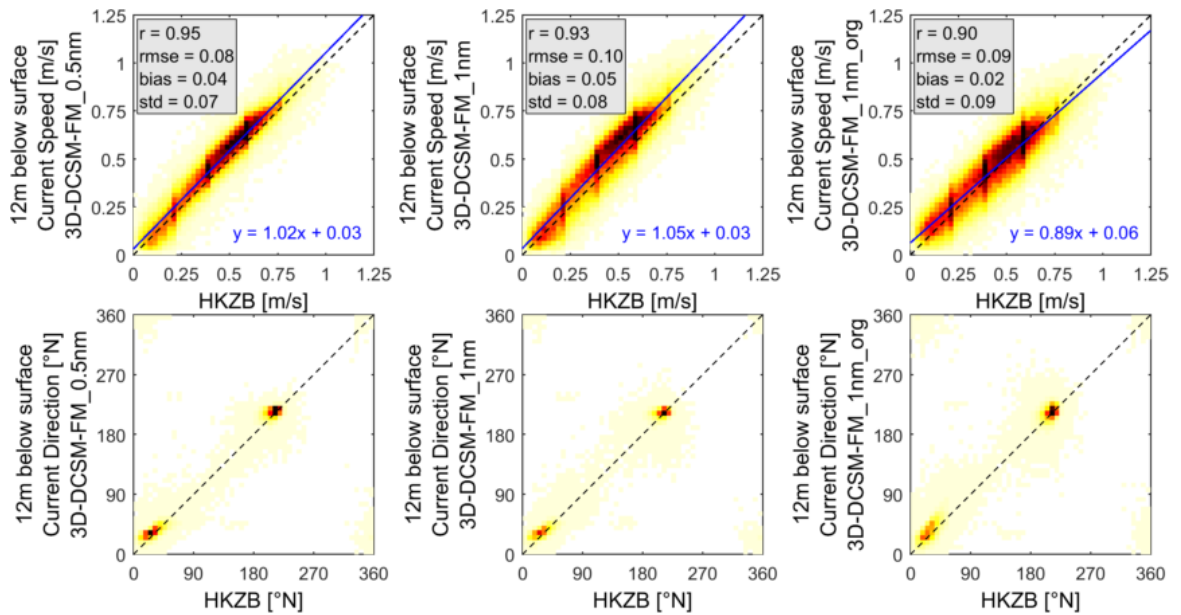


Figure 7.7 Scatter plots of current magnitude and direction at **12 m below the surface** at station **HKZB_WS158** for the period June 2016 to December 2017 (left: 0.5 nm; middle: 1 nm; right: original).

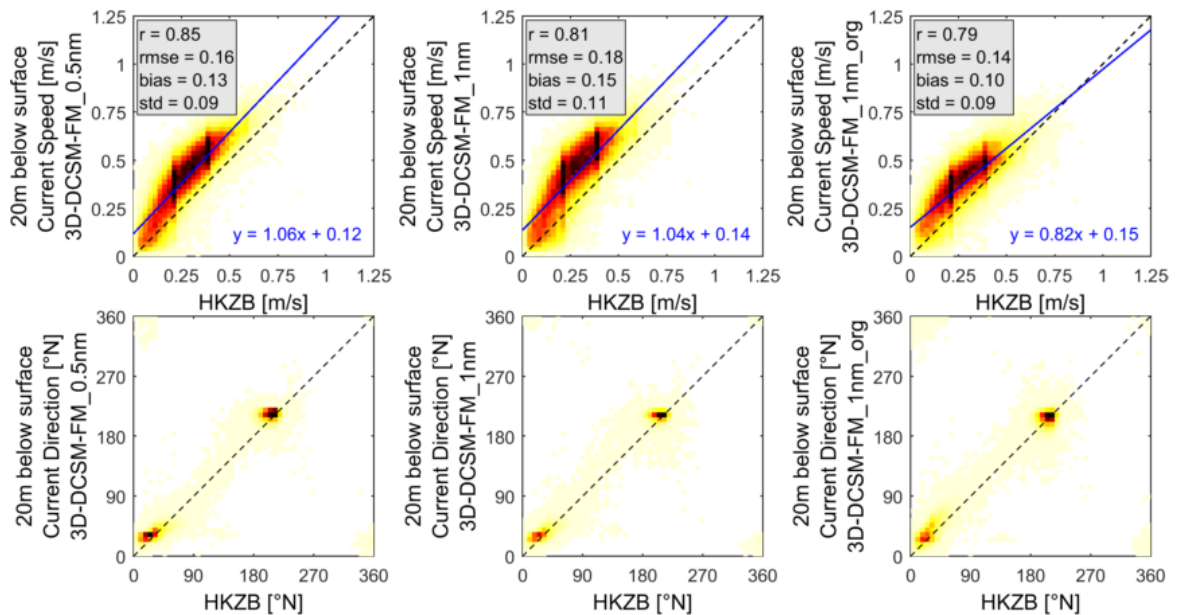


Figure 7.8 Scatter plots of current magnitude and direction at **20 m below the surface** at station **HKZB_WS158** for the period June 2016 to December 2017 (left: 0.5 nm; middle: 1 nm; right: original).

7.2.3 Variation over depth

The goodness-of-fit statistics in Table 7.2 show variation over depth. For the magnitude, the depth-averaged statistics are always better than the magnitudes near the bottom and the water surface. The statistics for the middle of the water column (12 meters below the water surface), are often close to the depth-averaged values. This indicates that although the depth-averaged values are simulated quite accurately, the shape of the velocity profile is not the same in model and measurements. To check this, the time-averaged velocity magnitude profiles are determined for both model and measurements. Note that the measurements in

the upper part of the water column are sometimes missing, probably due to the vertical tide. In this analysis layers are ignored if more than 10% of the data is missing. Because the use of sigma-coordinates in the model, the modelled profiles are given at vertical locations that vary in time (due to changing water levels). To generate the averaged modelled profiles, the water level is assumed to be constant (at the average water level).

The resulting average profiles are plotted in Figure 7.3 (HKZA) and Figure 7.4 (HKZB). These figures show that the model overestimates the average current velocity magnitude in the entire water column. This is especially the case at the lower most measurement position at station HKZB. While most profiles show monotonously increasing current magnitudes, this is not the case for the average profiles measured profile at HKZA. There, a small decrease is visible between 13 m and 15 m from the bottom. Furthermore, the lowermost measured value at HKZB deviates significantly for the value directly above. This raises the question whether these lower data are accurate.

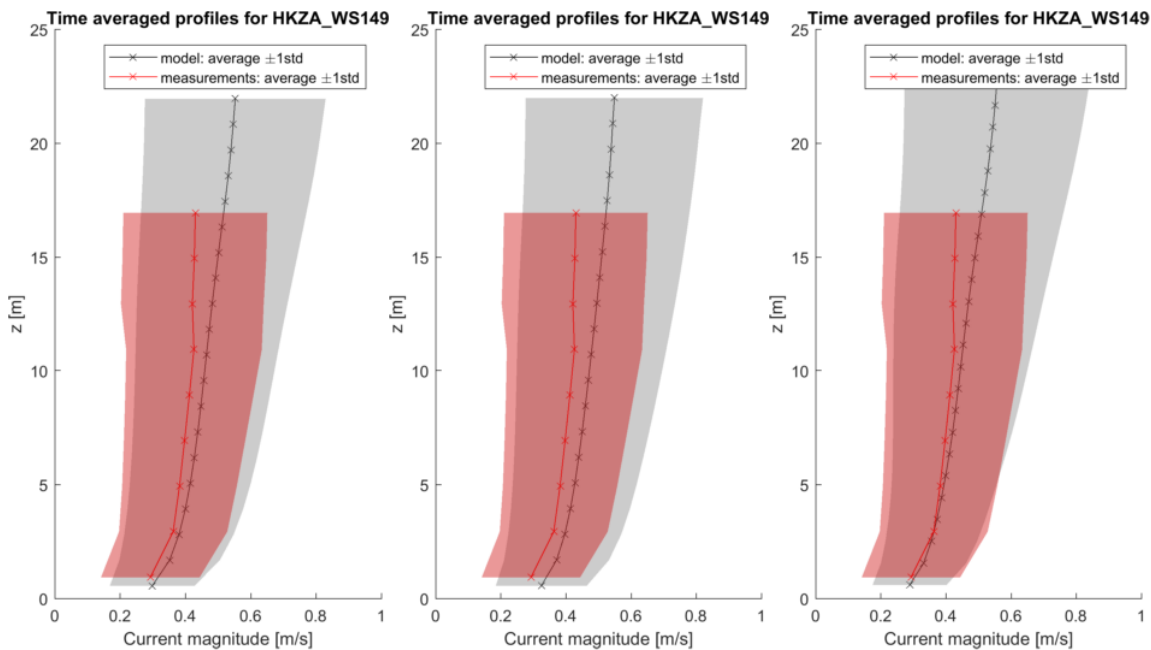


Figure 7.9 Modelled (grey) and measured (red) time-averaged current magnitude profile at station **HKZA** for the period June 2016 to December 2017 (left: 0.5 nm; middle: 1 nm; right: original).

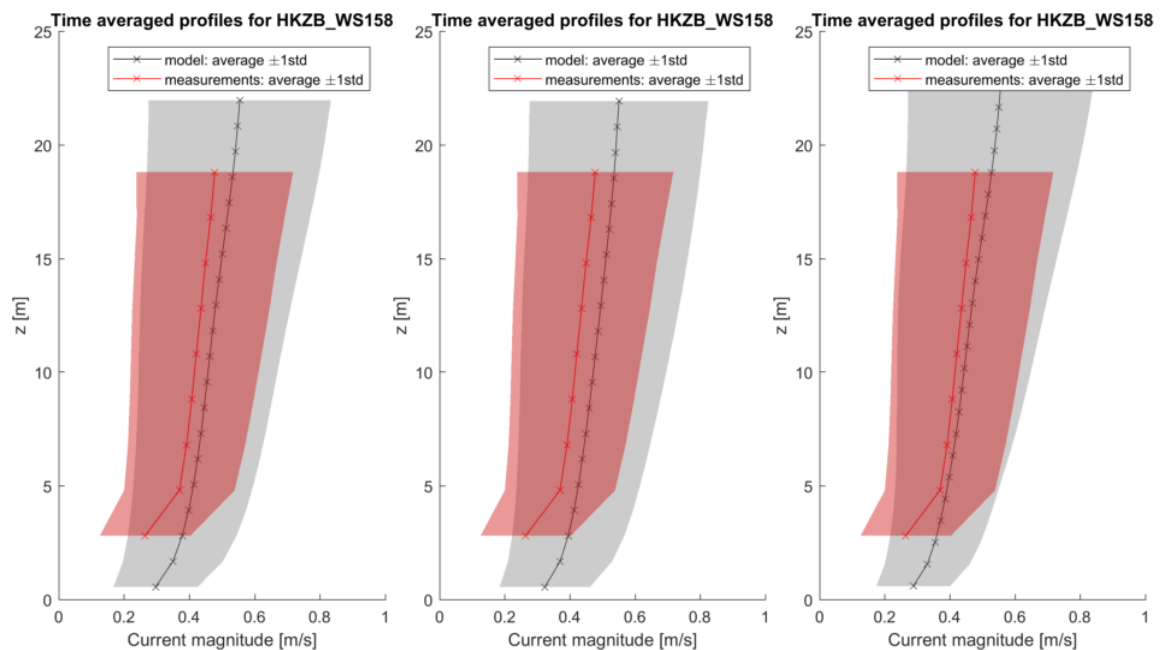


Figure 7.10 Modelled (grey) and measured (red) time-averaged current magnitude profile at station **HKZB** for the period June 2016 to December 2017 (left: 0.5 nm; middle: 1 nm; right: original).

7.3 Kustgenese 2 Ameland data

7.3.1 Visual comparison

Figure 7.11 to Figure 7.13 show time series of the model (0.5 nm) and measurements for an arbitrary one-week period. In these figures the velocity vector is split in a magnitude and the direction. Current directions for velocity magnitudes lower than 0.2 m/s are ignored in all plots and subsequent analysis.

These figures show that the model often underestimates peak velocities at station MF-04-A. At station MF-06-A (located further offshore), the magnitude of the peak velocities is more or less correct. The timing of the most severe overestimations suggests that the cause is not tidal in nature. Temporary variation in fresh water discharge might play a role. In this respect it should be noted that the actual fresh water discharges were not available in this period (2017) and that climatological monthly mean values have been used. Another potential cause of is the absence of interaction between currents and waves in the model.

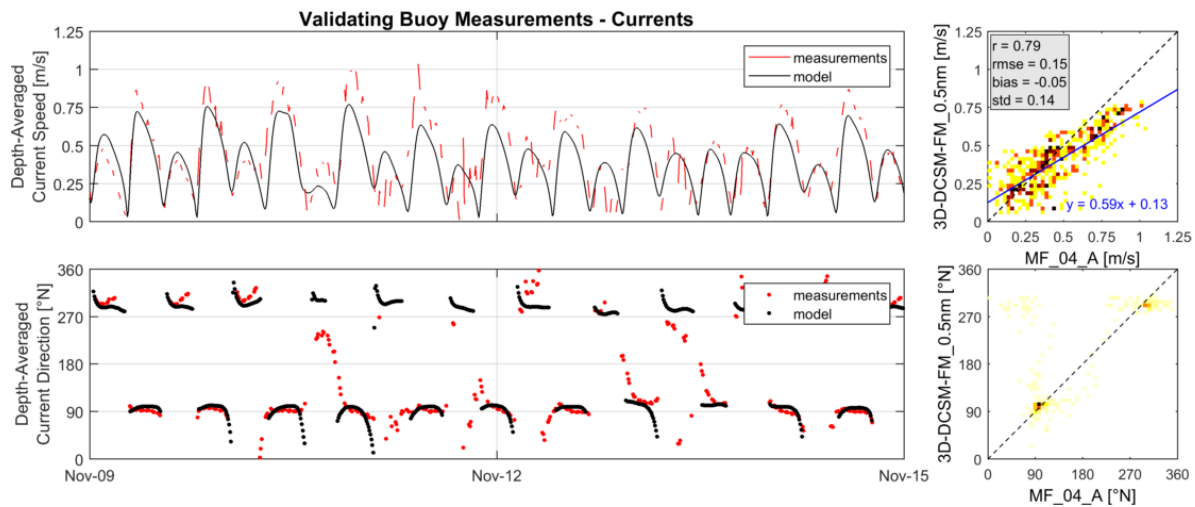


Figure 7.11 Time series of measured and modelled (3D DCSM-FM 0.5 nm) depth-averaged current magnitude and direction for station **MF-04-A** for an arbitrary one-week period.

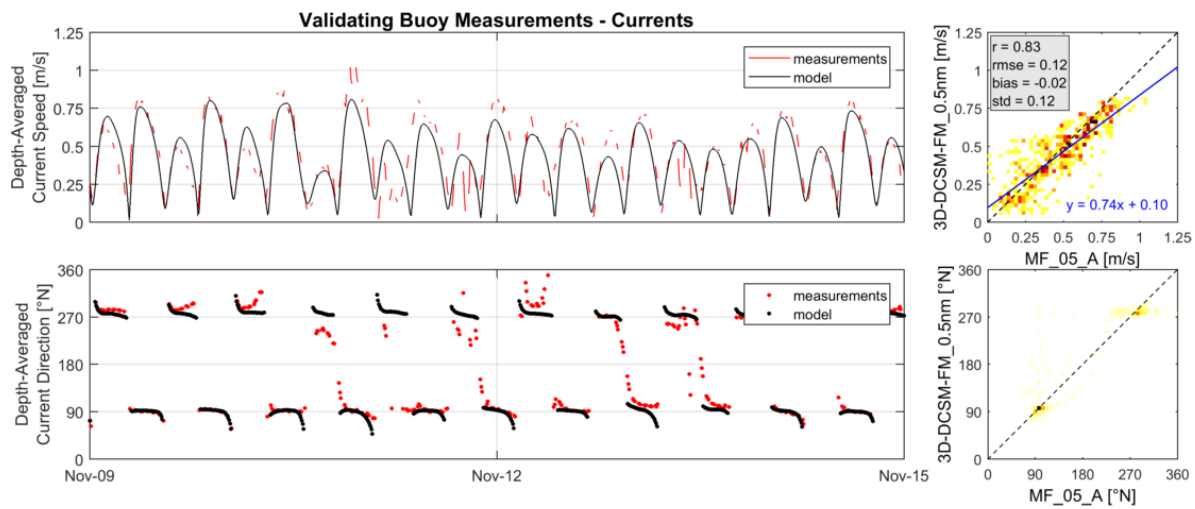


Figure 7.12 Time series of measured and modelled (3D DCSM-FM 0.5 nm) depth-averaged current magnitude and direction for station **MF-05-A** for an arbitrary one-week period.

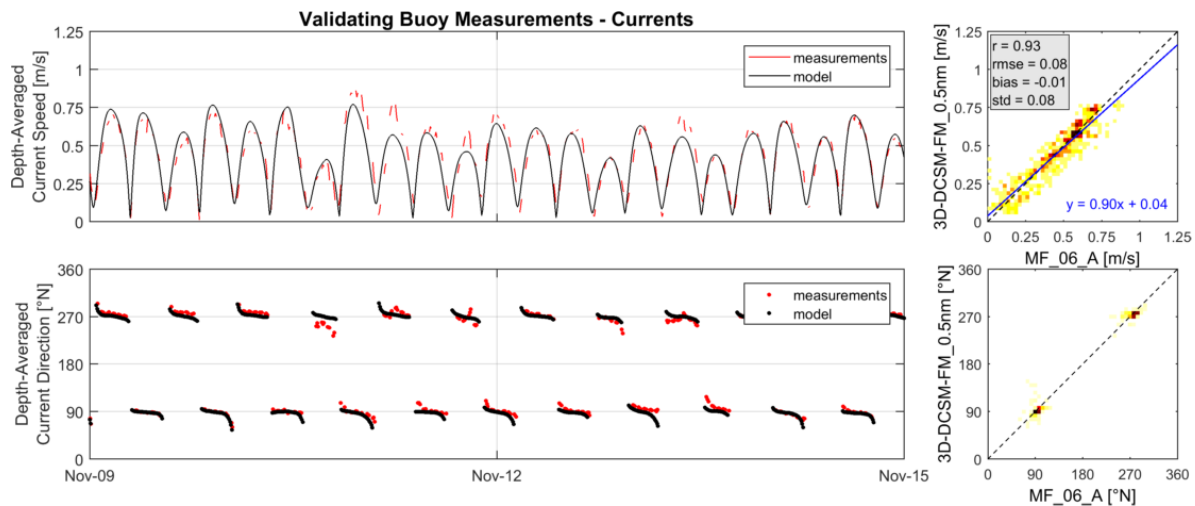


Figure 7.13 Time series of measured and modelled (3D DCSM-FM 0.5 nm) depth-averaged current magnitude and direction for station **MF-06-A** for an arbitrary one-week period.

7.3.2 Quantitative comparison

In order to quantitatively compare the results for the different model configurations and measurement locations, all statistics are summarized in Table 7.3. The accompanying scatter plots are presented in Figure 7.14 (MF-04-A), Figure 7.15 (MF-05-A), Figure 7.16 (MF-06-A). The results in these tables and figures represent the comparison for the period for which measurements are available (November-December 2017).

The results in the table make clear that the 0.5 nm configuration of the model systematically underestimates the velocity magnitude at all three stations. This is indicated with negative values for the bias, ranging from -0.6 cm/s at MF-04-A to -0.1 cm/s at MF-06-A). The other two configurations show a small systematic overestimation (ranging from 0.1 to 0.4 cm/s). With respect to the correlation coefficient, the standard deviation and the RMSE, the 0.5 nm configuration shows the best level of accuracy. Clearly, the increased resolution has a beneficial impact, especially at the most nearshore location (MF-04-A).

It should be noted that the measurements considered are located at a complex area, not necessarily representative of the larger scale processes along the Dutch coast. In the original and 1 nm configuration location MF-04-A and MF-05-A are located in the same model cell, and MF-06-A is one cell apart (see Figure 7.2), even though the measurements show considerable differences.

Table 7.3 Summary of the statistics of the data-model comparison for Kustgenese 2 Ameland locations (MF-04-A, MF-05-A and MF-06-A) for the period November to December 2017.

Model		0.5 nm	1 nm	org
Depth [m]		DA	DA	DA
MF-04-A	magnitude R [-]	0.83	0.70	0.76
	RMSE [m/s]	0.15	0.18	0.16
	bias [m/s]	-0.06	0.02	0.02
	std [m/s]	0.14	0.18	0.16
MF-05-A	magnitude R [-]	0.86	0.84	0.84
	RMSE [m/s]	0.12	0.13	0.13
	bias [m/s]	-0.03	0.02	0.01
	std [m/s]	0.12	0.13	0.13
MF-06-A	magnitude R [-]	0.92	0.93	0.92
	RMSE [m/s]	0.08	0.09	0.10
	bias [m/s]	-0.01	0.03	0.04
	std [m/s]	0.08	0.08	0.09

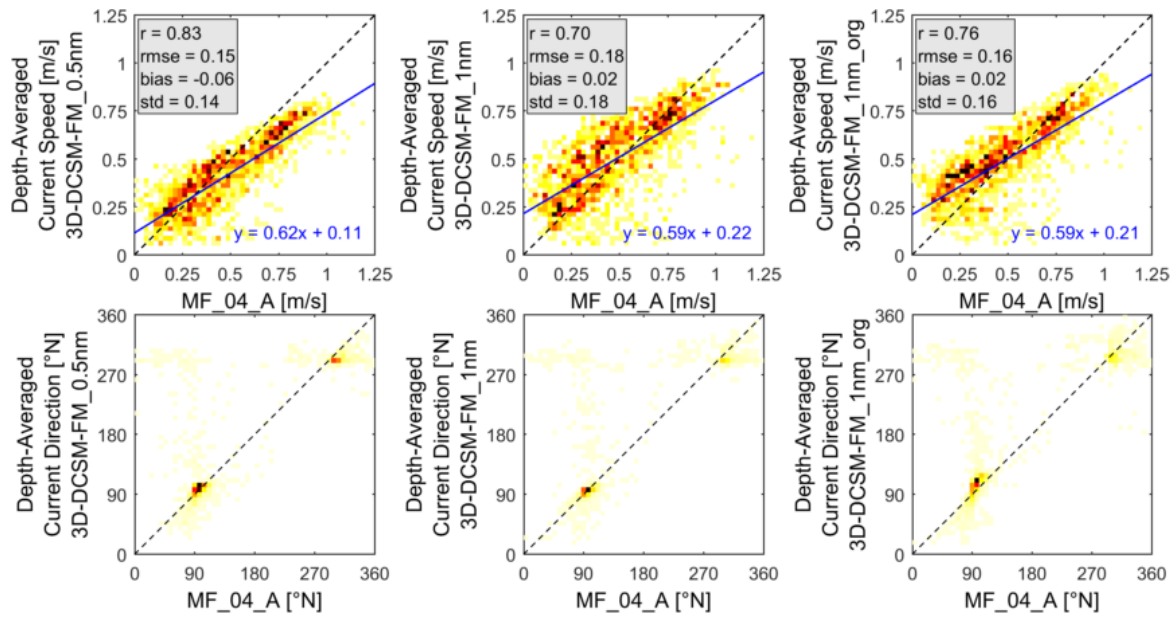


Figure 7.14 Scatter plots of **depth-averaged** current magnitude and direction at station MF-04-A for the period November-December 2017 (left: 0.5 nm; middle: 1 nm; right: original).

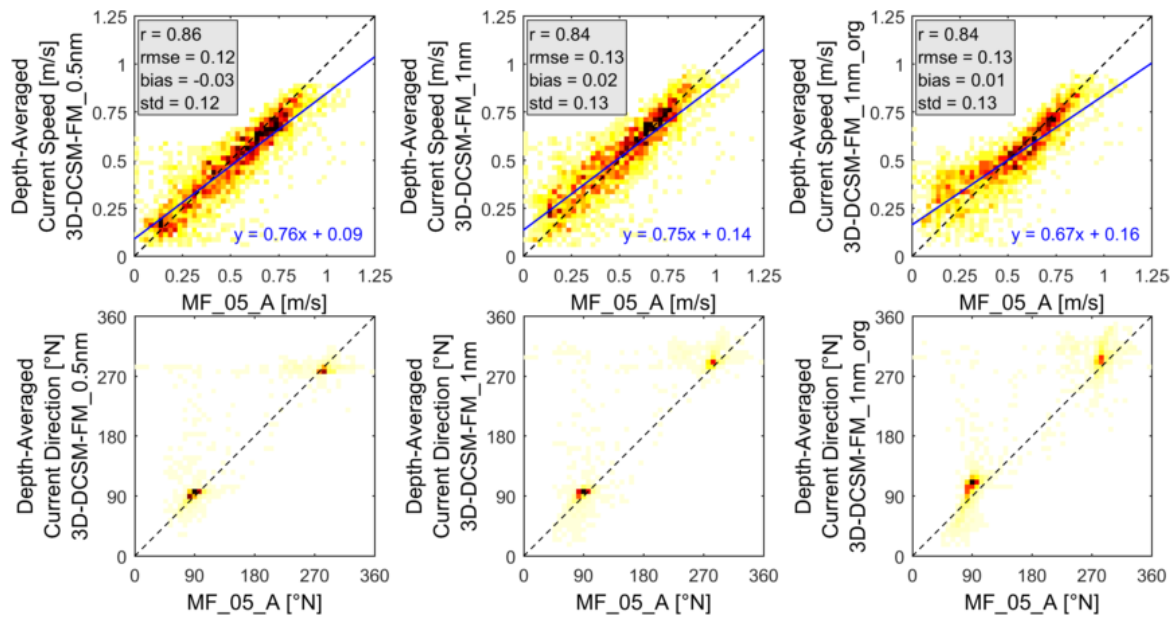


Figure 7.15 Scatter plots of **depth-averaged** current magnitude and direction at station MF-05-A for the period November-December 2017 (left: 0.5 nm; middle: 1 nm; right: original).

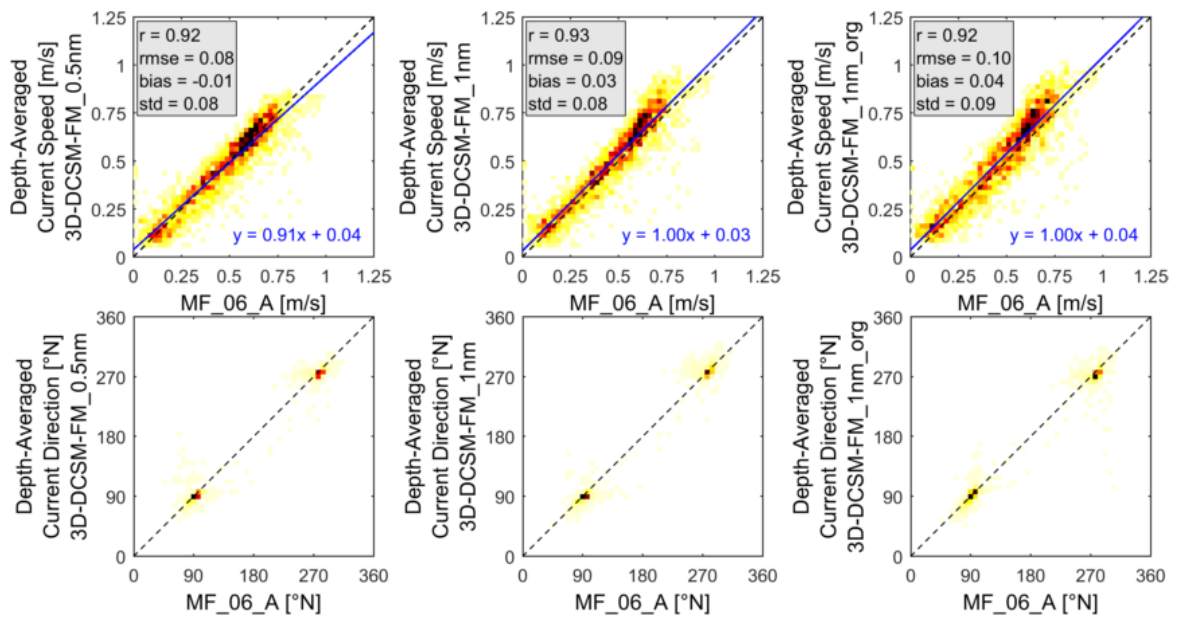


Figure 7.16 Scatter plots of **depth-averaged** current magnitude and direction at station MF-06-A for the period November-December 2017 (left: 0.5 nm; middle: 1 nm; right: original).

7.3.3 Variation over depth

The average profiles for these three stations are plotted in Figure 7.17 (MF-04-A), Figure 7.18 (MF-05-A) and Figure 7.19 (MF-06-A). Because stations MF-04-A and MF-05-A are in the same model cell of the original and 1 nm configuration, the model results are the same for these stations (in the 0.5 nm configuration each station is in a separate cell). For station MF-04-A in the 1 nm model, the water depth from the model and measurement are very different, indicating that the bathymetry changes cannot be captured in the coarse model cells. This station also shows an overestimation for the 0.5 nm model, which is absent in the 1 nm model. The vertical velocity profile of station MF-06-A is represented most accurately in the 0.5 nm model configuration.

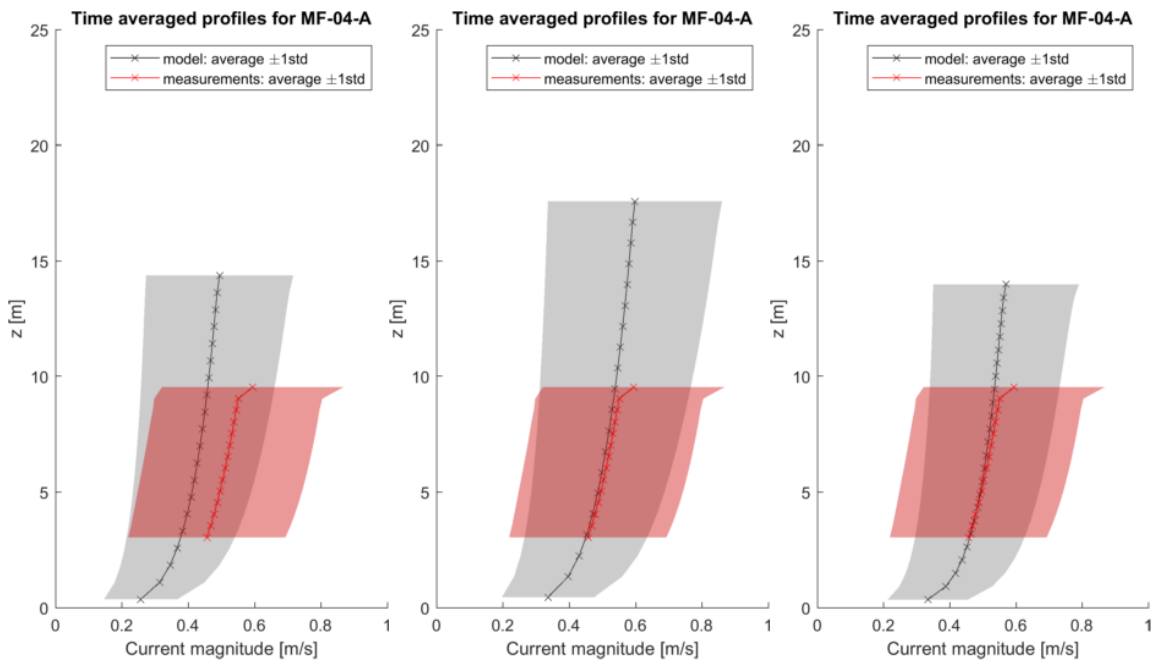


Figure 7.17 Modelled (grey) and measured (red) time-averaged current magnitude profile at station **MF-04-A** for the period November to December 2017 (left: 0.5 nm; middle: 1 nm; right: original).

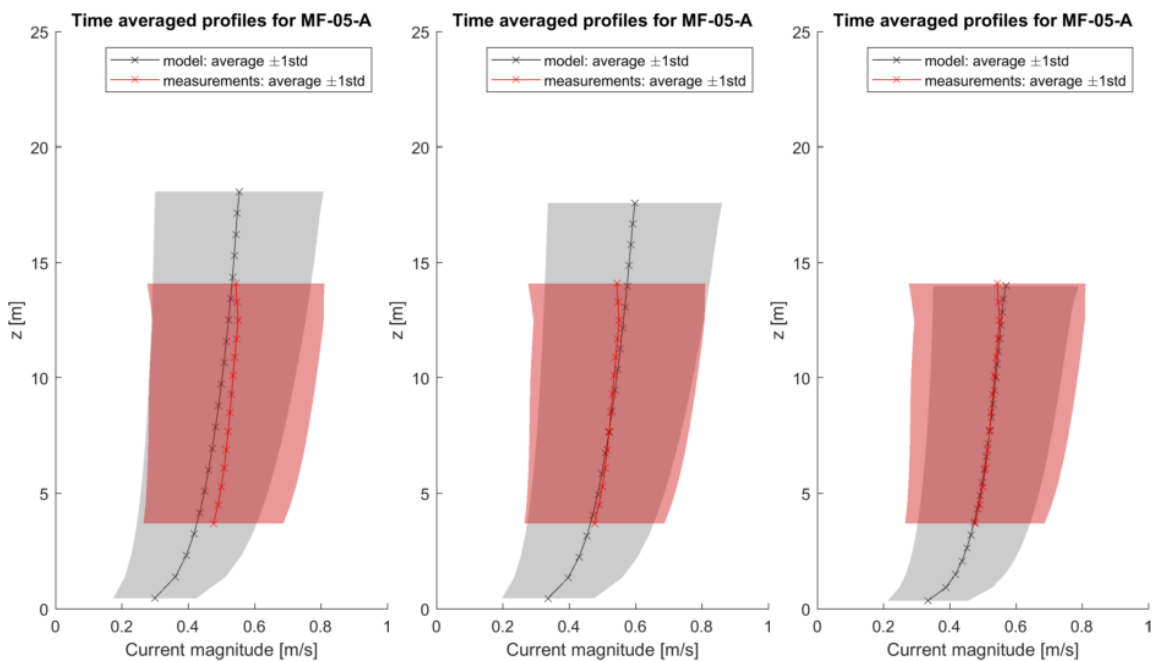


Figure 7.18 Modelled (grey) and measured (red) time-averaged current magnitude profile at station **MF-05-A** for the period November to December 2017 (left: 0.5 nm; middle: 1 nm; right: original).

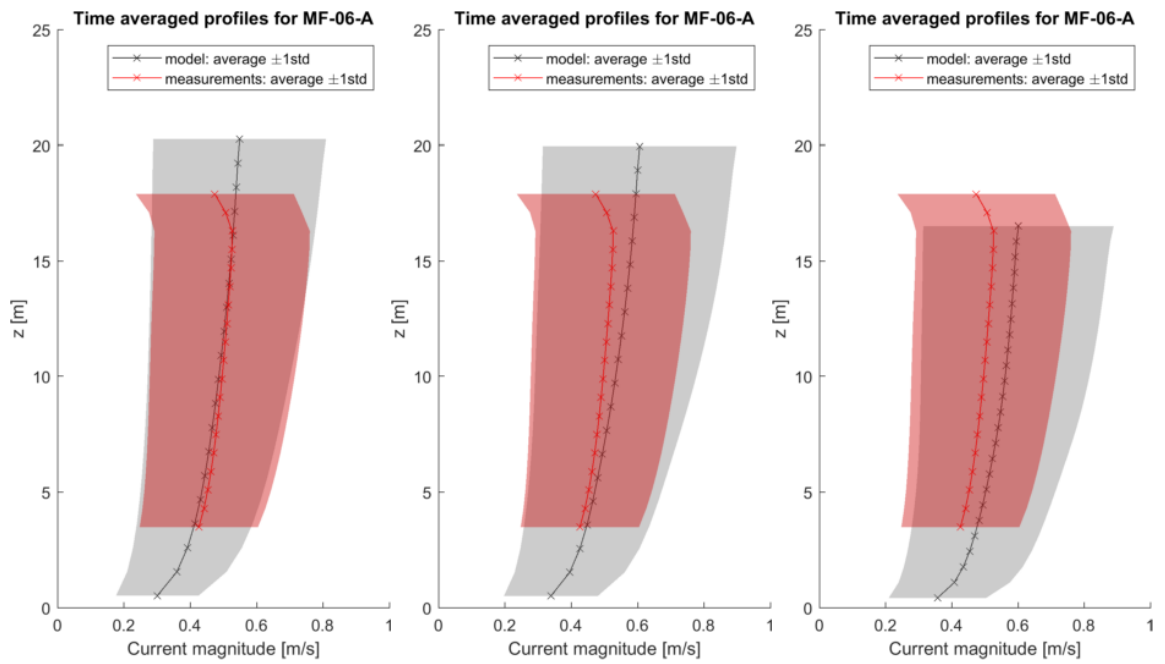


Figure 7.19 Modelled (grey) and measured (red) time-averaged current magnitude profile at station **MF-06-A** for the period November to December 2017 (left: 0.5 nm; middle: 1 nm; right: original).

8 Conclusions and recommendations

8.1 Conclusions

This report describes the model setup and validation of the 3D Dutch Continental Shelf Model developed in D-HYDRO Flexible Mesh (3D DCSM-FM). The validation is performed for three configurations of the model, which differ from each other with respect to (a.o.) horizontal resolution, model bathymetry and bottom roughness and are referred to as:

- 'original' configuration
- '1 nm' configuration
- '0.5 nm' configuration

One of the main advantages of the latter two schematizations is that the bathymetry is based on an improved data product (EMODnet; in the original configuration adjusted NOOS bathymetry was used, see paragraph 1.3). This has removed the need to adjust the model bathymetry during the model calibration. While this adjustment was beneficial for the skill with which water levels are represented, it is unclear what the impact on current velocities is.

Water levels

- Validation for the calendar years 2013-2015 at a selection of 13 stations along the Dutch coast shows an average total water level RMSE of 9-10 cm for all three configurations. Although differences are relatively small, the 0.5 nm version is slightly better than the 1 nm version, while the original configuration produces the best results in terms of total water levels.
- It was shown that the tide representation quality has reduced in comparison to a 2D barotropic version of the model. This is presumably partly caused by double counting in imposing the annual seasonal cycle S_a in the 3D model.
- Despite the above, 3D DCSM-FM still model performs substantially better than the official ZUNO-DD model (maintained by Rijkswaterstaat), with a decrease in tide, surge and total water level errors by more than 50%.

Water temperature

- The sea surface temperature is well represented. This holds specifically for the inter-annual variability as well as the spatial variation of the seasonal amplitude.
- The average bias, std and RMSE in the stations assessed are 0.4-0.5 °C, 0.5-0.6 °C and 0.7-0.8 °C, respectively.
- Even though in the central North Sea there is a good match with measured sea surface temperatures, at the bottom the rate of increase in spring temperatures is underestimated. This leads to an overestimation of the temperature stratification, with the largest mean overestimation (0.8 °C) present in 3D DCSM-FM 0.5 nm.

Surface salinity

- A quantitative assessment of the sea surface salinity representation at the Noordwijk and Terschelling transect shows that the original configuration yields salinities that are generally lower than the other two configurations.
- The impact of resolution is limited at the Terschelling transect, while at the Noordwijk transect the bias decreases from 0.9 psu to 0.6 psu by an increase in resolution to 0.5 nm.
- The simulation with increased horizontal resolution exhibits more temporal variation in salinity. This is probably related to the finer spatial scales that can be resolved on a higher resolution grid.

- The cross shore gradient at the Noordwijk and Terschelling transect is more or less well represented, with the original setup having a gradient that is somewhat too steep and the other two configurations showing less fresh water nearshore.

Residual transport through the English Channel

- There is considerable inter-annual variation in residual transport, ranging from $70 \cdot 10^3 \text{ m}^3/\text{s}$ to $180 \cdot 10^3 \text{ m}^3/\text{s}$ in the 0.5 nm version.
- In the original configuration the mean transport ($97 \cdot 10^3 \text{ m}^3/\text{s}$) is around the value commonly thought to be accurate, without the need to artificially adjust the open boundaries (as was the case in the 3D ZUNO-DD model). On average the 1 nm and 0.5 nm configuration yield residual transports that are ~20% larger than the original configuration.
- The horizontal model resolution (0.5 nm vs. 1nm) has limited impact on the mean residual transport.

Current speed

- All three configurations of the model overestimate the depth-averaged velocity magnitude at stations HKZA (by 2-3 cm/s) and HKZB (by 6-7 cm/s), both located 27 to 28 km offshore from the Egmond coast. However, the standard deviation of the magnitude error is generally lowest for the 0.5 nm configuration. This also holds for the correlation coefficient and implies that the current representation improves by increasing the model resolution from 1 nm to 0.5 nm.
- Comparison with the Kustgense-2 measurements near Ameland shows that with respect to the correlation coefficient, the standard deviation and the RMSE, the 0.5 nm configuration shows the best level of accuracy. Clearly, the increased resolution has a beneficial impact, especially at the most nearshore location (MF-04-A).
- Visual inspection shows that the model often underestimates peak velocities at station MF-04-A. At station MF-06-A (located further offshore), the magnitude of the peak velocities is more or less correct. The timing of the most severe overestimations suggests that the cause is not tidal in nature.

8.2 Recommendations

- It is recommended to improve the boundary conditions by replacing the barotropic annual Sa forcing with a steric correction based on the already prescribed time-varying salinity and temperature profiles at the open boundaries. After changing this, the impact on the results presented in the present report - in particular the residual transport through the English Channel - should be assessed.
- The bias in sea surface temperature in Anasuria is double the average bias in other stations. This is mainly due to an underprediction of winter temperatures, which might be related to a poorer temperature representation in deeper water. It is recommended to assess the sensitivity to a better vertical grid schematization off the shelf (e.g. by using a combination of strictly horizontal layers in the lower part of the water column and sigma-coordinates near the surface).
- The overestimation of temperature stratification in the central North Sea points to a lack of vertical mixing. It is therefore recommended to assess the sensitivity to the vertical background eddy diffusivity values.
- It is recommended to make a more thorough comparison against the quality of the ZUNO-DD model, which currently is the official 3D RWS model for the southern North Sea. A brief comparison for water levels provided in the present report suggests substantial improvements with the 3D DCSM-FM model.

- It is recommended to further validate the model against the other current measurements that are available (cf. Table 7.1).
- The timing of the most severe overestimations of current magnitude at the Kustgenese 2 Ameland measurement suggests that the cause is non-tidal in nature. Temporary variation in fresh water discharge might play a role. In this respect it should be noted that the actual fresh water discharges were not available in this period (2017) and that climatological monthly mean values have been used. It is recommended to redo this part of the validation once time-varying discharge rates for 2017 are available. Furthermore, it is recommended to extend the number of discharge locations with actual discharges in the Wadden Sea (e.g. Lauwersmeer) and include a better estimate of the associated water temperature. Currently a constant mean value of 11 °C is used. Another cause might be a lack in spatial resolution and the absence of interaction between currents and waves in the model.

References

- Charnock, H., 1955. Wind stress on a water surface. Quarterly Journal of the Royal Meteorological Society, 81(350), 639-640.
- Grasmeijer, B., 2018. Method for Calculating Sediment Transport on the Dutch Lower Shoreface. Report 1220339-000-ZKS-041. Deltares, Delft, The Netherlands.
- Lodder, Q., 2016. Rekenregel suppletievolumen. Rijkswaterstaat Memo.
- Zijl, F., Verlaan, M., Gerritsen, H., 2013. Improved water-level forecasting for the Northwest European Shelf and North Sea through direct modelling of tide, surge and non-linear interaction. Ocean Dyn. 63 (7).
- Zijl, F., Groenenboom, J., 2017. Development of a 6th generation model for the NW European Shelf. Report 11200570-004-ZKS-0002. Deltares, Delft, The Netherlands.